Structural Determinants for the Mode of Action of the Imidazopyridine DS2 at δ-containing γ-Aminobutyric Acid Type A ($GABA_A$) Receptors

Frederik Rostrup[†], Christina B. Falk-Petersen[†], Kasper Harpsøe[†], Stine Buchleithner[†], Irene Conforti[†], Sascha Jung[‡], David E. Gloriam[†], Tanja Schirmeister[‡], Petrine Wellendorph[†], Bente Frølund[†,]*

[†] Department of Drug Design and Pharmacology, Faculty of Health and Medical Sciences, University of Copenhagen, Universitetsparken 2, DK-2100 Copenhagen. [‡] Institute of Pharmaceutical and Biomedical Sciences, Johannes Gutenberg University Mainz, D-55128, Germany

KEYWORDS. Extrasynaptic $GABA_A$ receptors, δ-selectivity, $\alpha_4\beta_1\delta$, DS2, imidazopyridine, positive allosteric modulation, ago-PAM, FMP assay, computational modeling.

ABSTRACT

Despite the therapeutic relevance of the δ-containing $GABA_A$ receptors and the need for δ-selective compounds, insight into the structural determinants for the mode and molecular site of action of the δ-selective positive allosteric modulator imidazo[1,2-a]pyridine DS2 remains elusive. To guide the quest for insight we synthesized a series of DS2 analogs by introducing various synthetic chemistry approaches to structurally diversify the imidazopyridine scaffold guided by a structural receptor model. Using a fluorescence-based FLIPR membrane potential assay we found that the δ-selectivity and the pharmacological profile in terms of allosteric agonistic or modulatory effect of the compounds are severely affected by substituents in the 5-position of the imidazopyridine core scaffold. Interestingly, the 5-methyl, 5-bromo and 5-chloro DS2 analogs, **30**, **35** and **36** were shown to be superior to DS2 at $\alpha_4\beta_1\delta$ as mid-high nanomolar potency δ-selective allosteric modulators, displaying 6–16 times higher potency than DS2. Of these, **30**, also displayed at least 60 times selectivity for $\alpha_4\beta_1\delta$ over $\alpha_4\beta_1\gamma$ receptor subtypes. Interestingly, the corresponding 5-iodo analog, **33**, displayed a dual allosteric agonistic and positive allosteric modulatory profile (ago-PAM). In conclusion, our study illustrates how even subtle modifications to the imidazypyridine scaffold of DS2 can give rise to diverse pharmacological profiles and inform the details of the binding site. Furthermore, the identified compound **30** has potential for the selective characterization of δ-containing $GABA_A$ receptors in general.

INTRODUCTION

γ-aminobutyric acid (GABA) is the major inhibitory neurotransmitter in the central nervous system[1] and mediates its effect via the ionotropic $GABA_A$ receptors ($GABA_ARs$) and the metabotropic $GABA_B$ receptors.[2] The $GABA_ARs$ are clinically employed targets for numerous drugs including anesthetics[3], barbiturates[4] and benzodiazepines[5] for their sedative, anxiolytic and anticonvulsant effects. $GABA_ARs$ form transmembrane heteropentameric complexes from at least 19 different subunits including α_{1-6}, β_{1-3}, γ_{1-3}, ρ_{1-3}, δ, θ, π and ε.[6] The combination of subunits affects the subcellular localization and type of inhibition being mediated. The majority of $GABA_ARs$ has the general stoichiometry of 2α, 2β and 1γ subunits and are typically located synaptically mediating fast and transient inhibition.[7] The synaptic $GABA_ARs$ are sensitive to high concentrations of GABA and are prone to desensitization. However, in $GABA_ARs$ primarily located extrasynaptically, the γ-subunit has in most cases been replaced by a δ-subunit. These extrasynaptic $GABA_ARs$ are sensitive to low concentrations of GABA and mediate tonic inhibition, distinct from the fast and transient synaptic inhibition, and are less prone to desensitization.[8] As the δ-subunit-containing $GABA_ARs$ have been proposed to be implicated in e.g. alcoholism,[9] epilepsy[8] and major depression disorder,[10] these receptors have been in focus in the last decades as potential drug targets (for reviews, see e.g. Brickley and Mody (2012)[11]; Lee and Maguire (2014)[12]). To date, few compounds exhibit δ-selectivity[13, 14] including the imidazo[1,2-a]pyridine DS2 (Figure 1), shown by Jensen et al to be a functionally selective $\alpha_{4/6}\beta_3\delta$ positive allosteric modulator (PAM), relative to its action at $\alpha_4\beta_3\gamma_2$ and $\alpha_1\beta_3\gamma_2$ receptors.[15] In addition, DS2 has been shown to selectively modulate $\alpha_4\beta_{1/3}\delta$ over $\alpha_4\beta_{1/3}$ receptors in 1-10 μM concentrations. Although DS2 does not appear to pass the blood-brain-barrier (BBB) in rat and mice,[15] we recently reported uptake of a ^{11}C-labelled DS2 analog, [^{11}C]DS2OMe (Figure 1) into the pig brain.[16]

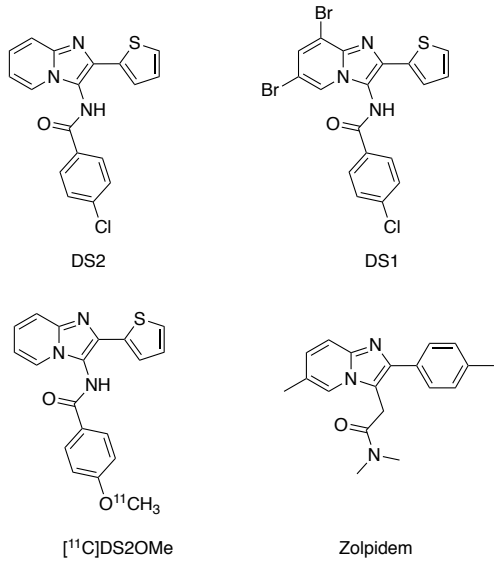

Figure 1. Chemical structures of the δ-selective $GABA_AR$ allosteric modulator, DS2, the PET ligand candidate, [^{11}C]DS2OMe, the allosteric $GABA_AR$ agonist, DS1 and the standard benzodiazepine binding site ligand zolpidem.

A previous structure-activity (SAR) study on the direct agonist effect of DS2 and the 6,8-dibromo analog, DS1 (Figure 1), reported that DS1, but not DS2, is able to increase [^{3}H]-ethynylbicyclooethobenzoate ([^{3}H]-EBOB) binding to δ-containing $GABA_ARs$ in the absence of GABA.[17] EBOB is a potent non-competitive $GABA_AR$ antagonist that binds to the picrotoxinin-binding site within the $GABA_AR$ ion channel.[18] [^{3}H]-EBOB binding is sensitive to conformational changes in the chloride-conducting channel, which can be mediated by increasing concentrations of GABA and/or affected by modulators in the presence or absence of GABA.[19-21] In the referred SAR study, two DS1 analogs were identified as δ-selective allosteric agonists in the absence of GABA.[17] However, both compounds lost their δ-selectivity in the presence of GABA, thus limiting their use for *in vivo* studies.[17]

Despite DS2 being an important tool compound,[14, 22, 23] and regardless of extensive investigations, its molecular site of action remains elusive[3, 15]. Herein, we describe our efforts to investigate the

molecular determinants for the pharmacology of DS2 at $\alpha_4\beta_1\delta$ $GABA_A$Rs by probing the δ-selective modulatory effect on the activity of GABA using a fluorometric imaging plate reader (FLIPR) membrane potential (FMP) functional assay. Ultimately, we sought to assist future modeling and site-directed mutagenesis studies that could lead to the revelation of the undiscovered DS2 binding site.[15, 17] Consequently, we expand the pharmacophore for the δ-selective allosteric effect on GABA modulation by introducing various synthesis strategies to structurally diversify the imidazopyridine scaffold of DS2 including a structural receptor model.

RESULTS AND DISCUSSION

Ligand Design

Based on the structural similarity between DS2 and the standard benzodiazepine binding site ligand zolpidem (Figure 1), we hypothesized that DS2 may bind in a benzodiazepine-like binding pocket at the inter-subunit α_4/δ-interface at $\alpha_4\beta_1\delta$ $GABA_A$Rs. This extracellular domain (ECD) pocket has been referred to as the C-loop pocket,[24] and the existence of such a pocket at δ-containing $GABA_A$Rs has previously been debated.[15, 25] The binding hypothesis is further challenged by the subunit stoichiometry and assembly of δ-$GABA_A$Rs, which continues to be poorly understood.[26-29]

To rationally guide ligand design, we constructed a homology model of the ECD C-loop pocket at the α_4/δ-interface using the cryo-EM structure of the human $\alpha_1\beta_2\gamma_2$ $GABA_A$R in complex with flumazenil (PDB-code: 6D6T)[30] as a template for our model. This model was subsequently used for induced fit and XP-Glide docking of previously reported compounds[17]. The putative binding mode obtained for DS2 (Figure 2A-B) predicts the following specific interactions: i) charge-assisted hydrogen bonds from the central amide to α_4R135 and δE71, ii) π-cation interaction from the imidazo[1,2-a]pyridine to δR157 and δH204, iii) π-stacking between the chlorophenyl and δF90.

Additionally, other surrounding amino acids delineate the binding site, which are considered as a van der Waals surface, some in direct contact and some further away allowing space for substituents.

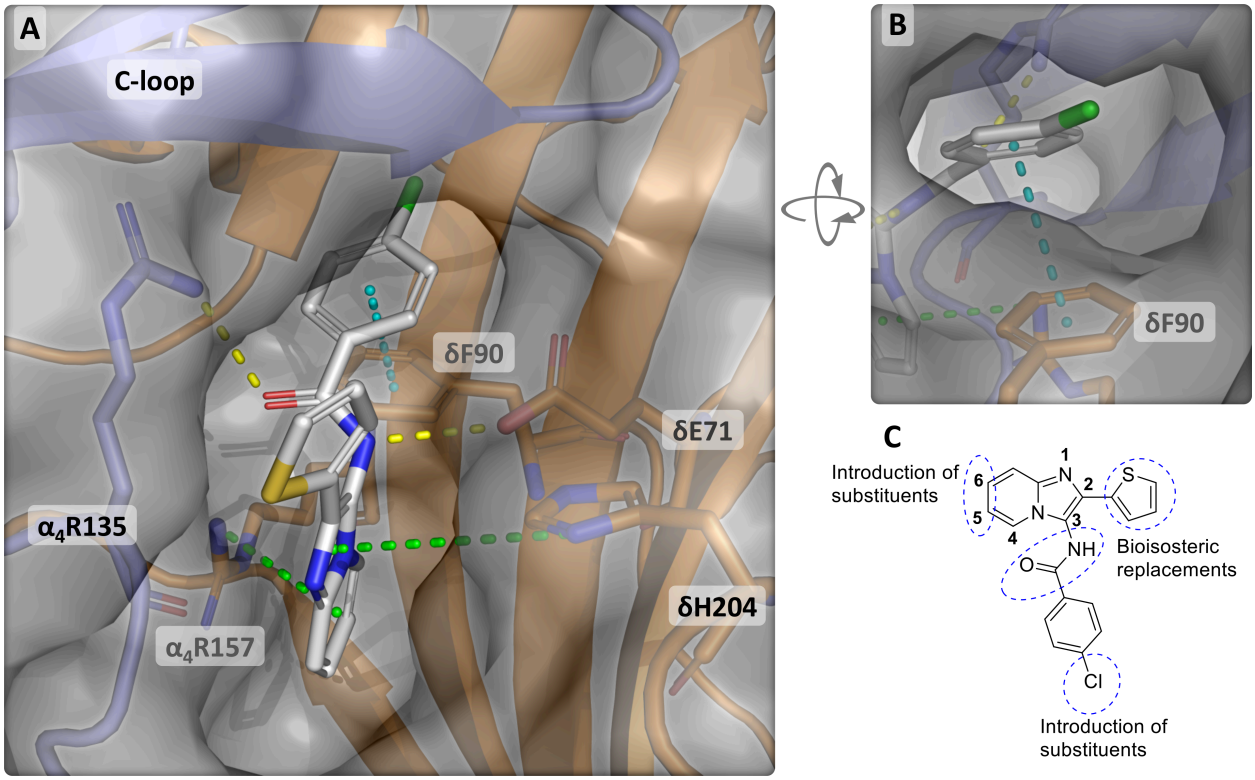

Figure 2. A and **B**) Putative binding model of DS2 (white carbon atoms) in the extracellular part of the $GABA_AR$ interface between the α_4 (purple carbon atoms) and δ (orange carbon atoms) subunits showing charge-assisted hydrogen bonds, π-cation and π-π interactions between DS2 and the receptor (yellow, green and cyan dotted lines, respectively), highlighted in another view in **B**). The amino acid backbone of $GABA_AR$ is depicted as cartoon and selected residues as sticks, while the van der Waals surface is shown in transparent grey. Besides the carbon atoms, which are colored according to molecules, oxygen, nitrogen, sulphur and chlorine are red, blue, yellow and green, respectively. **C**) Schematic overview of the explored sites in the DS2 scaffold and numbering of the positions.

To test the predicted binding mode, we systematically varied the structural scaffold of DS2, as depicted in figure 2C. If our predicted binding mode is true, the amide functionality in position 3 (Figure 2C) with both a hydrogen bond donor and acceptor function should be crucial to modulation, which can be probed by bioisosteric replacement, exemplified by compounds **40** and **42** (Scheme 4). To this end, we examined the lack of aromatic interactions to the thiophene in position 2 (Figure 2C), and the available space from almost protruding out of the binding site by increasing the aromatic ring

size and removing the aromaticity by compounds **18** and **22** (Schemes 1 and 2). Likewise, the chlorophenyl of DS2 is predicted to point into an unexplored area under the C-loop and even out from the binding site leaving space for substituents (Figure 2B), which was challenged by compound **25** (Scheme 3). In contrast, the binding mode model show limited to a fair amount of room for substitution possibilities in the 6- and 5-position of the imidazo[1,2-a]pyridine, which was explored by compounds **27**, **28**, **30**–**36** (Scheme 3).

Synthesis of Target Compounds

The new DS2 analogues **24**–**34** and **40** were synthesized as depicted in Schemes 1-4. Compound **35** and **36** were synthesized according to procedures reported in the literature.[17]

Scheme 1. Imidazo[1,2-a]pyridine-3-amine synthesis via GBB-multicomponent reaction[a]

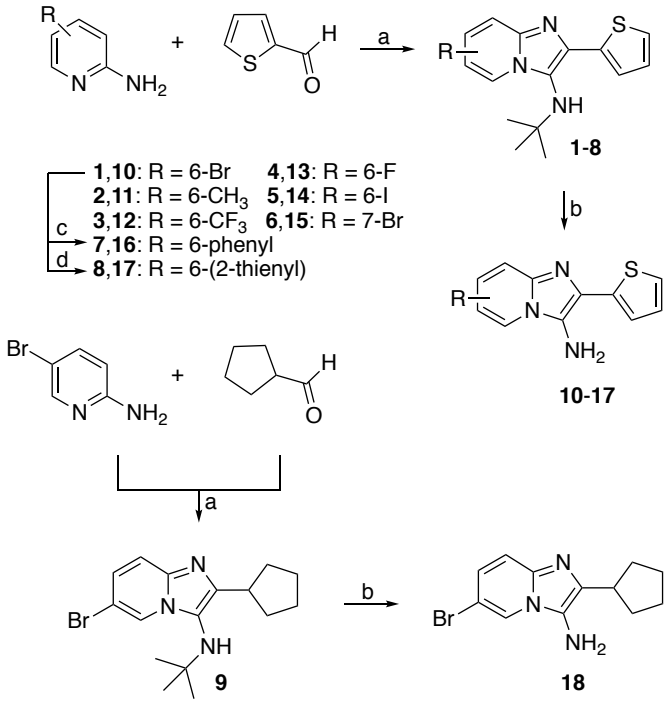

[a]Reagents and conditions: (a) *tert*-butyl isocyanide, NH_4Cl, toluene, reflux; (b) 5M HBr, 110 °C. (c) $Pd(PPh_3)_4$, Na_2CO_3, $PhB(OH)_2$, DME/H_2O, reflux. (d) $Pd(PPh_3)_4$, Na_2CO_3, 2-ThienylB$(OH)_2$, DME/H_2O, reflux .

The 2-substituted imidazo-[1,2-a]pyridin-3-amides (**24–34**) were all achieved in a two-step procedure via the corresponding amines (**10**–**18**). Initially, a one-step Groebke–Blackburn–Bienayme (GBB) multicomponent reactions[31-33] with potassium cyanide, the respective 2-aminopyridines, aldehydes and different Lewis acids were attempted to achieve **10**. However, by-product formation, including formation of bicondensated adducts[34] and poor starting material conversion resulted in low yields and unsuccessful workups. Alternatively, the *tert*-butyl protected intermediates, imidazo-[1,2-a]pyridine-3-amines (**1**–**9**), were obtained in medium to high yield through similar GBB multicomponent reactions[31-33] using the appropriate substituted 2-aminopyridines, *tert*-butyl isocyanide and commercial available aliphatic or aromatic aldehydes (Scheme 1). To introduce aromatic moieties into the pyridine ring, the bromide in **1** was used as a handle in a Suzuki-Miyaura cross-coupling reaction with commercially available boronic acids, affording **7-8** in decent yield (52-60%). Subsequent acidic deprotection using hydrobromic acid afforded the intermediate amines **10**–**18**.

Scheme 2. Synthesis of 2-substituted Imidazo[1,2-a]pyridine-3-amine [a]

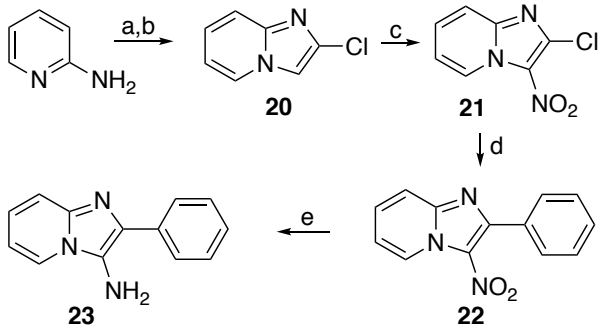

[a]Reagents and conditions: (a) 2-chloroacetic acid, Et_3N/H_2O, 90 °C to give 2-(2-iminopyridin-1(2*H*)-yl)acetic acid (**19**); (b) $POCl_3$, toluene, reflux; (c) Conc. H_2SO_4, HNO_3, 5°C to rt.; (d) $Pd(PPh_3)_4$, DME/H_2O, $NaCO_3$, reflux; (e) $SnCl_2$, MeOH, reflux.

To expand the flexibility of the design and diversity of the substituents, a complementary strategy was explored based on a key intermediate, **21**, containing a chloride as a handle enabling introduction of an array of substituents in the 2-position of the imidazo[1,2-a]pyridine core scaffold (Scheme 2).

The intermediate **21** was synthesized according to procedures reported,[35] followed by a Suzuki-Miyaura cross-coupling affording the corresponding 2-phenyl analog, **22**, in high yield (88%). To explore a broader use of **21** for further structural elaboration, we showed that **21** readily undergo nucleophilic aromatic substitution with morpholine at room temperature in high yield (not shown). However, as others before us[36, 37], we encountered difficulties controlling the apparent substituent dependent outcome of the reduction of the nitro group. Moreover, the isolation of the resulting amine, under the given reaction conditions, proved complicated. In our hands, using tin(II)chloride in refluxing methanol proved to be the most feasible method and gave the desired amine **23**.

Finally, the 2-substituted imidazo-[1,2-a]pyridin-3-amides (**24–34**) were obtained from the corresponding amines, **10**–**18** and **23**, and the appropriate acyl chlorides in a mixture of toluene and pyridine (Scheme 3). Multiple of the amides proved troublesome to purify using standard column chromatography purification methods. However, classical methods such as trituration or recrystallization afforded the pure target compounds.

Scheme 3. Synthesis of N-(2-substituted Imidazo[1,2-a]pyridin-3-yl)amides [a]

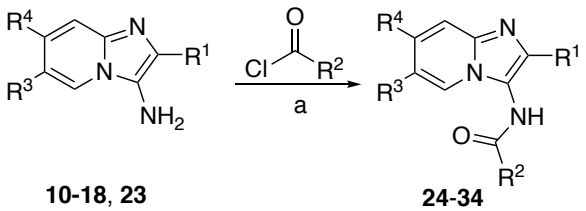

10-18, **23** **24-34**

cmp	R^1	R^2	R^3	R^4
24	2-thienyl	Ph	Br	H
25	2-thienyl	4-PhO-Ph	Br	H
26	cyclopentyl	Ph	Br	H
27	2-thienyl	Ph	Ph	H
28	2-thienyl	Ph	2-thienyl	H
29	Ph	Ph	H	H
30	2-thienyl	4-Cl-Ph	CH_3	H
31	2-thienyl	4-Cl-Ph	CF_3	H
32	2-thienyl	4-Cl-Ph	F	H
33	2-thienyl	4-Cl-Ph	I	H
34	2-thienyl	4-Cl-Ph	H	Br
35	2-thienyl	4-Cl-Ph	Cl	H
36	2-thienyl	4-Cl-Ph	Br	H

[a]Reagents and conditions: (a) Toluene/pyridine, rt. The table shows the structural details of the synthesized compounds **24**–**34**. Compounds **35** and **36** have been reported previously[17]

The amide bioisosteres, 1,2,3-triazole and 1,2,4-oxadiazole, were obtained as illustrated in Scheme 4. The imidazo[1,2-a]pyridine core scaffold of the intermediates **37** and **38** was synthesized through an initial alkylation-condensation reaction using 2-bromo-1-phenylethan-1-one.

Scheme 4. Synthesis of amide bioisosteres of DS2 [a]

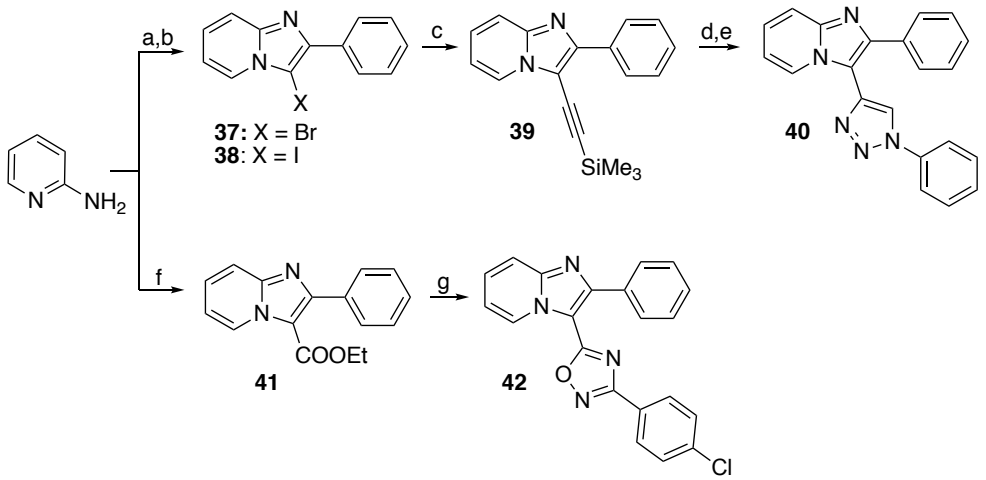

[a]Reagents and conditions: (a) 2-bromo-1-phenylethan-1-one, $NaHCO_3$, MeOH, reflux; (b) MeCN, NBS for X = Br, NIS for X = I, rt; (c) TMSA, $Pd(PPh_3)_2Cl_2$, CuI, Et_3N, 80 °C; (d) TBAF, THF, rt.; (e) phenylazide, $CuSO_4 \cdot 5H_2O$, sodium ascorbate, THF/H_2O, rt; (f) ethyl 3-oxo-3-phenylpropanoate, CBr_4, MeCN, 80 °C; (g) 4-chloro-*N*'-hydroxybenzimidamide, DMSO, NaOH, rt.

To introduce a handle for the subsequent cross-coupling reaction affording **39**, a regioselective halogenation using *N*-bromo- or *N*-iodosuccinimide was performed to give **37** and **38**, respectively in high yield.[38] Subsequent Sonogashira cross-coupling followed by a TBAF mediated deprotection gave access to the terminal alkyne. Interestingly, we found that the bromo analog, **37**, was superior to the iodo analog, **38**, as cross-coupling partner, according to yield of compounds obtained, as dehalogenation was observed when using the latter. Finally, the 1,2,3-triazole was installed through a copper-catalyzed alkyne-azide cycloaddition (CuAAC) which furnished **40** in 78% yield.

The ester **41** was prepared as previously described[39] using ethyl 3-oxo-3-phenylpropanoate and subsequent cyclocondensation with 4-chloro-*N*'-hydroxybenzimidamide[40] affording the 1,2,4-oxadiazole **42**.

Structure-Activity Relationship of the Target Compounds at $\alpha_4\beta_1\delta$ and $\alpha_4\beta_1\gamma_2$ $GABA_A$Rs. The compounds were subjected to functional characterization in the FMP assay. Initially, the compounds were tested in a single concentration of 10 μM as agonists at $\alpha_4\beta_1\delta$ and $\alpha_4\beta_1\gamma_2$ $GABA_A$Rs and as PAMs (applied together with a concentration of GABA corresponding to EC_{20}), to evaluate intrinsic activity as well as selectivity (Figure 3).

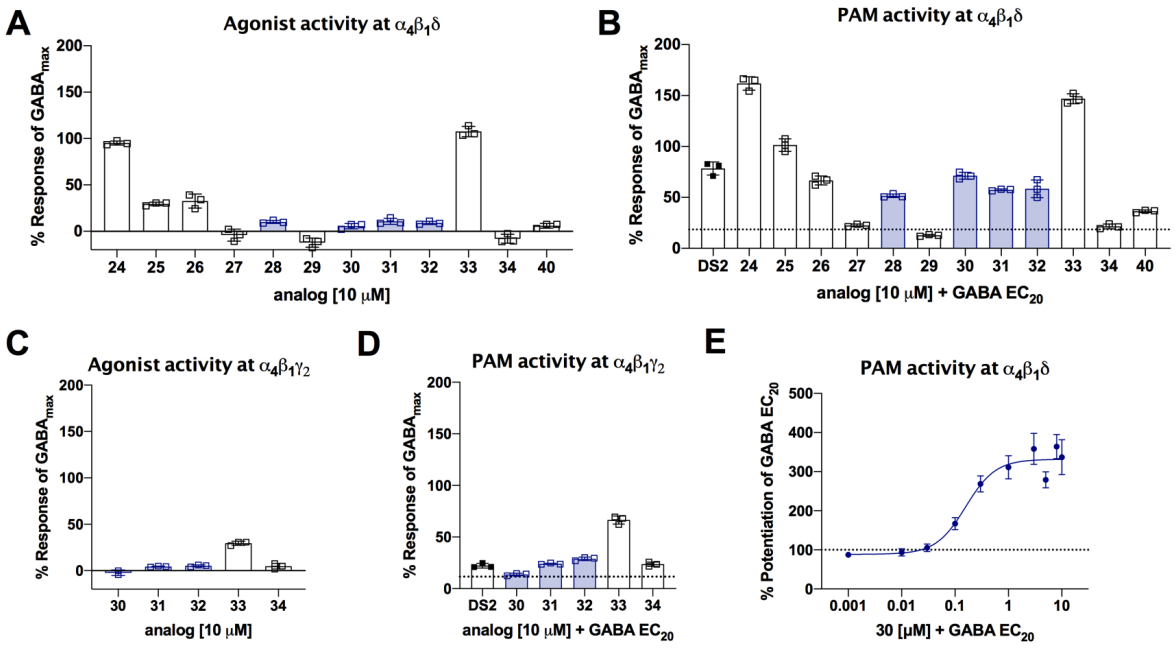

Figure 3 Initial testing of agonist and PAM activity of compounds **24–34** and **40** at $\alpha_4\beta_1\delta$ and compounds **30–34** at $\alpha_4\beta_1\gamma_2$ receptors. Agonist activity of 10 μM of the compounds at **A)** $\alpha_4\beta_1\delta$ and **C)** $\alpha_4\beta_1\gamma_2$. PAM activity induced by 10 μM of the compounds at **B)** $\alpha_4\beta_1\delta$ and **D)** $\alpha_4\beta_1\gamma_2$ in the presence of GABA (EC_{20}, see table 2). E) Concentration-response curve showing the PAM activity of **30** at $\alpha_4\beta_1\delta$. The data are shown as means±SD. Data in **A**), **B**) and **E**) are representative from two-three independent experiments and data shown in **C**) and **D**) are from a single experiment. The dotted line represents the response from GABA EC_{20} co-applied with the analogs, when testing the PAM activity in **B**), **D**) and **E**). Selected compounds investigated further are highlighted in blue.

The compounds **27**, **29**, and **34** were found to have no activity at $\alpha_4\beta_1\delta$ and were therefore not pursued further. In addition, the poor solubility of the 1,2,4-oxadiazole (**42)** precluded the compound from pharmacological characterization. Compounds **24–26** and **33** demonstrated agonist activity as these compounds induced responses at $\alpha_4\beta_1\delta$ in the absence of GABA, making these compounds ago-PAMs. However, since we were primarily interested in PAMs, these were not characterized further. Instead, compounds **28** and **30–32** were singled out as displaying no or limited agonist activity (Figure 3B). The most efficacious of these, **30–32**, were further indicated to display some selectivity for $\alpha_4\beta_1\delta$ over $\alpha_4\beta_1\gamma_2$ (Figure 3D). The bioisosteric replacement of the amide with a triazole was tolerated as **40** revealed PAM activity at $\alpha_4\beta_1\delta$, although seemingly with a relatively low efficacy.

The two most efficacious agonists, **24** and **33**, in this study display potent modulatory effects as well (Figure 3A,B). However, the SAR obtained for the modulatory effect on GABA activity, in this specific study and described previously[17], seems to differ from the corresponding SAR for the allosteric agonist effect. This is especially pronounced for the 5-substituted analogs **28** and **30–32**, showing significant modulatory effect but no direct agonist effect.

Next, we generated full concentration-response curves of the 5-methyl, 5-trifluoromethyl and 5-fluoro DS2 analogs **30–32** in the presence of GABA (EC_{20}) (Figure 3E, Table 2). In addition, due to significant structural overlap, we included the previously identified 5-chloro and 5-bromo DS2 analogs, **35** and **36**, in this series as well.[17] The determined EC_{50} values of the PAM activities are shown in Table 2. The methyl analog **30** was found to stand out both in terms of potency and selectivity. It displayed a PAM potency of 160 nM (EC_{50}) (Figure 3E) which is approximately 6 times higher than DS2 itself at $\alpha_4\beta_1\delta$. Additionally, **30** showed no activity at 10 μM at $\alpha_4\beta_1\gamma_2$ (>60 times selectivity for $\alpha_4\beta_1\delta$). Compound **35** and **36** were equally potent as **30** but lacked the same degree of

selectivity. Compounds **31** and **32** were neither more potent than DS2 itself at $\alpha_4\beta_1\delta$, nor did they match the selectivity observed for DS2.

Table 2. PAM potencies of selected DS2 analogs.

	EC_{50} (μM), [pEC_{50} ± SEM], n			
Compound	$\alpha_4\beta_1\delta$		$\alpha_4\beta_1\gamma_2$	$\alpha_1\beta_2\gamma_2$
DS2	0.98	[6.01±0.078], 4	- [c]	- [c]
30	0.16	[6.79±0.082], 4	>10; n=3[a]	- [c]
31	1.10	[5.96±0.063], 3	n=2[b]	- [c]
32	1.92	[5.72±0.046], 3	n=2[b]	- [c]
35	0.14	[6.84±0.140], 5	- [c]	n=2[b]
36	0.060	[7.22±0.079], 4	- [c]	n=2[b]

Concentration-response curves were obtained in the FMP assay. Compounds were co-applied with a concentration of GABA corresponding to approximately GABA EC_{20} determined from full GABA concentration-response curves at the respective receptors. Concentrations used to induce EC_{20} response were: $\alpha_4\beta_1\delta$: 0.06 μM, $\alpha_4\beta_1\gamma_2$: 0.6 μM, and $\alpha_1\beta_2\gamma_2$: 0.5 μM. [a] No potentiation in the tested concentration range 0.01-10 μM. [b] Small potentiation for concentrations higher than 1 μM. Not able to fit data to a sigmoidal curve. [c] Not tested.

Structural Rationalization of Major SAR Observations.

The fact that we observe slight potentiation of GABA responses at γ-containing receptors for some of our compounds (Table 2) may seem contradictory to a binding site in the $\alpha_4\delta$ subunit interface. However, considering the possibility of weak binding to a corresponding binding site in a $\alpha_{1/4}\gamma_{2S}$ subunit interface, the resulting SAR was still interpreted in reference to our proposed binding model for DS2 in the $\alpha_4\delta$ subunit interface (Figure 2). The 5-position (R^3) in the pyridine part of the scaffold (Figure 2C) was investigated in most detail, and proved to be important for the δ-selectivity of the compounds. This is evident as **30**–**32**, containing a methyl, trifluoromethyl or a fluorine at this position, potently potentiated $\alpha_4\beta_1\delta$ responses, while exhibiting no or negligible activity at $\alpha_4\beta_1\gamma_2$ (Table 2). Surprisingly, the iodinated compound **33,** as the only of this series, was shown to be a dual allosteric agonist and modulator at both $\alpha_4\beta_1\delta$ and $\alpha_4\beta_1\gamma_2$ (Figure 3 and Table 2). Additionally, as demonstrated by the apparently differential effects on potentiation vs. activation (Figure 3; **33** vs. **30**

and **24** vs. **25**), the 5-position together with R^2 substituents may be used to optimize the PAM activity over allosteric agonism or vice versa. In contrast to the markedly diminished allosteric agonist effect, the retained PAM activity of **25** with the 4-OPh instead of the 4-Cl in the parent compound, DS2, is consistent with our predicted binding model showing additional available space for substitution (Figure 2B), this clearly indicates further R^2-substitution possibilities and warrants additional future investigation of other and even bigger and more bulky substituents in this position. For the 5-position (R^3), a 5-membered ring seem to be the largest allowed, as the 2-thienyl (**28**) retains PAM activity while a phenyl substituent (**27**) no longer potentiates the GABA EC_{20} response (Figure 3). Again, these results are consistent with our model showing available space at the 5-position (Figure 2A).

Though only a single compound explores R^4 substitution (**34**), the lack of effect with a bromo-substituent in this specific position corroborates with the fairly tight fit between DS2 and the receptor in our model, predicting very limited space for substitution. However, when it comes to the lack of activity for **29** (Figure 3), which has an R^1 phenyl substituent, our model fails to provide an explanation. No apparent specific interactions were obtained in the docking and there seem to be ample space for the slightly larger phenyl compared to the 2-thienyl. However, it is tempting to speculate from our pharmacological results that this part of the compounds should bind in a tight pocket encompassing a 5-membered ring, also non-aromatic (**26**), but no larger than that. On the other hand, compound **40**, which shows moderate PAM activity, has a phenyl in the corresponding position on a scaffold with a triazole bioisostere replacing the amide. Thus, it could also be the common absence of an R^3 substituent that causes the lack of potentition by **29** and **34**. Further studies are needed to investigate this. Additionally, the triazole bioisoteric replacements of the amide (**40**) conflicts with the binding mode of DS2 as it is unable to form both of the charge-assissted hydrogen bonds observed for the amide to α_4R135 and δE71, bridging the two subunits across the interface.

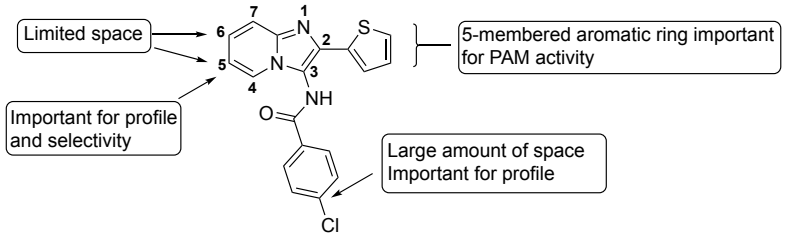

Figure 4. A summarized SAR for the DS2 scaffold in terms of δ-selective allosteric modulation.

Based on the above SAR analysis (summarized in Figure 4), where the pharmacological activity of the majority of the compounds agree, but a single compound contradicts our binding mode, it remains non-conclusive whether this is the site of action for DS2. To further investigate this hypothesis, structural guided site-directed mutagenesis studies are currently being analyzed in our lab.

Irrespective of our binding site hypothesis, our novel analogs of DS2 show that the 5-position of the scaffold is clearly vital for the pharmacological profile of the analogs (PAM/ago-PAM) as well as for the preference for $\alpha_4\beta_1\delta$ vs. $\alpha_4\beta_1\gamma_2$. Such dual activity is a known phenomenon,[41] where subtle structural differences result in diverse pharmacological activity profiles and selectivity as previously reported within the cys-loop receptor research field[42, 43].

CONCLUSIONS

In summary, we have synthesized a series of novel DS2 analogs through complementary synthesis strategies allowing structural diversification of the imidazopyridine core scaffold and identified novel compounds with better potency at, and higher selectivity for, δ-containing $GABA_A$Rs. We find that substituents in the 5-position of the imidazopyridine core scaffold severely affect both the δ-selectivity and modulatory activity. Interestingly, the 5-methyl, 5-bromo and 5-chloro DS2 analogs **30**, **35** and **36** are superior to DS2 at $\alpha_4\beta_1\delta$ as PAMS with 6- to 16 times increased potency, whereas

the structurally closely related 5-iodo analog, **33**, is an ago-PAM. This illustrates how even small differences in the imidazopyridine core scaffold of DS2, can give rise to diverse pharmacological profiles. Compound **30** provides a useful tool with improved sensitivity and selectivity for studying the specific subtype $\alpha_4\beta_1\delta$, recently proposed to have a functional role in the hippocampus[44] and possibly towards other δ-containing receptor subtypes.

EXPERIMENTAL SECTION

Chemistry.

General Procedures.

Melting points (mp) were determined on a SRS OptiMelt apparatus with open capillary tubes. The melting points are uncorrected. Triethylamine was stored over KOH pellets. TLC was performed on precoated silica 60 gel F_{254} from Merk and visualized at a UV-lamp at 254/366nm. Flash column chromatography was conducted manually in glass columns loaded with silica gel 60 (40 μm-63 μm) supplied by Merck. An internal solvent purification system provided anhydrous solvents as THF, DCM and DMF. Petroleum ether (PET) refers to the fraction boiling at 40-60°C. NMR spectra were obtained at 300K on either of two systems. A Bruker Avance II 400 MHz spectrometer equipped with a 5 mm broad band BBFO probe. Also, a Bruker Avance III HD 600 MHz spectrometer equipped with a 5 mm cryogenically cooled CPDCH $^{13}C(^{1}H)$Z-GRD probe was used. 16-64 scans were collected for ^{1}H-NMR spectra, depending on the concentration, with a relaxation delay of 1.0 sec. 256-3072 scans were collected for ^{13}C-NMR spectra using a relaxation delay of 2.0 or 4.0 sec. The solvent peak was used as the reference in which $CDCl_3$ (7.26 ppm and 77.16 ppm), MeOD-d_4 (3.31 ppm and 49.00 ppm), DMSO-d_6 (2.50 ppm and 39.52 ppm) was applied, respectively for ^{1}H- and ^{13}C-NMR. The obtained spectra were processed such as phase- and baseline corrected in MNova software, version 11.0. The spectral data is reported in the given order: Chemical shift (δ), multiplicity (singlet

(s), doublet (d) double doublet (dd), triplet (t), quartet (q), pentet (p), triplet of doublets (td), doublet of doublet of doublets (ddd), broad (b) and multiplet (m)), coupling constant(s) J(Hz), number of protons. The purity of the final compounds (≥95% unless otherwise stated) was determined on either of two HPLC systems. The samples were dissolved in 1 mL of (MeCN : H_2O)(1 : 1), or DMSO in cases in which the solubility of the compounds was found to be insufficient in (MeCN : H_2O)(1 : 1) and to avoid precipitation of the compounds on the column. HPLC system 1 was a LaChrome reversed phase system from Merck, Germany, Darmstadt that had a Chromolith SpeedROD RP-18 column (4.6 x 50 mm). Detection at 254 nm via an L-7400 UV detector. The samples were injected using an L-7200 auto sampler, injecting 1-10μL. An L7100 pump operating with either a flowrate at 3 or 4 mL/min was used. A linear gradient of A (99.9% H_2O : 0.1% TFA) and B (90% MeCN : 10% H_2O : 0.1% TFA) from 100% A to 90% B over 5 minutes was applied. The system used EZChromeElite software for data processing and collecting. HPLC system 2 was a Dioxnex Ultimate HPLC system which had a LPG-3400A pump with a flowrate at 1 mL/min, using the previously described mobile phases A and B. A linear gradient system from 100%A to 100% B over 15 minutes was used. 6 minutes column equilibration was performed after each run. The column was a Germini-NX C18 column (4.6 x 250 mm, 3μm, 110Å). A WPS-3000SL auto sampler was used, injecting 1-10 μL. This system had a DAD3000D diode array detector set to 225 nm, 240 nm, 254 nm and 290 nm. Data processing and collected was conducted using chromeleon software version 6.80. UPLC-ESI-MS was performed on a Agilent 1100 HPLC system equipped with an C-18 column (2.1mm x 50mm 1.7 μm), which was coupled to a Hewlett Packard 1100 series mass spectrometer with an electrospray ionization source was used. MassLynx mass spectrometry software version 4.1 was used for data processing. The samples were dissolved in 1 mL of (MeCN : H_2O) (1 : 1) and filtered through a 0.22 μm filter. The samples were injected via an Acquity FTN Autosampler. A flowrate of 0.8 mL/min was applied. A linear gradient system of A (MeCN : H_2O : HCOOH) (0.05 : 0.95 : 0.01) and

B (MeCN: HCOOH) (0.99: 0.01) which rose from 100 % A to 100 % B over 3.5 minutes and then 1 minute at 100%, maintaining a flowrate of 0.8 mL/min.

General Groebke-Blackburn-Bienaymé (GBB) procedure for *N*-(*tert*-butyl)-imidazo[1,2-a]pyridin-3-amines derivatives:

The aldehyde (1 equiv.) was dissolved in toluene (40-100 mL). NH_4Cl (1 equiv.), *tert*-butyl isocyanide (1.2 equiv.) and a 2-aminopyridine (1 equiv.) were then added in that order. The reaction mixture was heated to reflux under argon and monitored by TLC. The reaction mixture was cooled to room temperature, reduced *in vacuo* and reevaporated with 10 mL toluene to yield the crude product which was recrystallized to afford the pure *N*-(*tert*-butyl)-imidazo[1,2-*a*]pyridin-3-amines.

***N*-(*tert*-butyl)-6-bromo-2-(thiophen-2-yl)imidazo[1,2-*a*]pyridin-3-amine** (**1**). Obtained from 2-thiophenecarboxaldehyde (0.7 mL, 7.1 mmol), NH_4Cl (0.38 g, 7.1 mmol), *tert*-butyl isocyanide (1.0 mL, 8.4 mmol) and 2-amino-5-bromopyridine (1.24 g, 7.1 mmol), using the general GBB procedure. Additional *tert*-Butyl isocyanide (0.2 mL, 1.8 mmol) was added after 18 hours. The reaction mixture was refluxed for 48 hours in total. The crude product was recrystallized from (MeCN : H_2O) (16 : 1). The resulting solid was lyophilized to yield the product as white needles (2.31 g, 93%): mp 184 °C, R_f = 0.5 (DCM : EtOAc) (20 : 1). ^{1}H NMR (400 MHz, Chloroform-*d*) δ 8.34 – 8.29 (m, 1H), 7.56 (dd, *J* = 1.0 Hz, 1H), 7.44 – 7.38 (m, 1H), 7.33 (dd, *J* = 1.0 Hz, 1H), 7.17 (dd, *J* = 2.0 Hz, 1H), 7.10 (dd, *J* = 3.7 Hz, 1H), 3.09 (s, 1H), 1.19 (s, 9H). ^{13}C NMR (151 MHz, Chloroform-*d*) δ 139.68, 136.21, 134.87, 126.80, 126.52, 124.40, 124.25, 122.89, 122.27, 117.04, 105.51, 56.02, 29.70. ESI-MS (m/z) calculated $[M + H]^+$ for $C_{15}H_{16}BrN_3S$ = 350.03, found 350.0 and $[M + H + 2]^+$= 352.0.

***N*-(*tert*-butyl)-6-methyl-2-(thiophen-2-yl)imidazo[1,2-*a*]pyridin-3-amine** (**2**).[31] Obtained from 2-thiophenecarboxaldehyde (0.6 mL, 6.0 mmol), NH_4Cl (0.32 g, 6.0 mmol), *tert*-butyl isocyanide (0.8 mL, 7.1 mmol) and 2-amino-5-methylpyridine (0.65 g, 6.0 mmol) using the general GBB

procedure. The reaction mixture was refluxed for 23 hours. The crude product was recrystallized from (MeCN : H_2O) (3 : 10), which furnished the product as a grey crystalline solid, (1.03 g, 60% yield): mp 193-194 °C. R_f = 0.6 (PET : EtOAc) (1 : 1). ^{1}H NMR (400 MHz, Chloroform-*d*) δ 7.98 – 7.95 (m, 1H), 7.56 (dd, *J* = 3.6, 1.2 Hz, 1H), 7.42 (dd, *J* = 9.1, 1.0 Hz, 1H), 7.29 (dd, *J* = 5.1, 1.2 Hz, 1H), 7.09 (dd, *J* = 3.6 Hz, 1H), 6.97 (dd, *J* = 9.1, 1.7 Hz, 1H), 3.06 (s, 1H), 2.33 (s, 3H), 1.18 (s, 9H). ^{13}C NMR (151 MHz, Chloroform-*d*) δ 141.46, 138.02, 134.83, 127.57, 127.37, 124.76, 124.70, 122.77, 121.35, 121.07, 116.73, 56.84, 30.70, 18.57.

***N*-(*tert*-butyl)-2-(thiophen-2-yl)-6-(trifluoromethyl)imidazo[1,2-a]pyridin-3-amine** (**3**). Obtained from 2-thiophenecarboxaldehyde (0.9 mL, 9.3 mmol), NH_4Cl, (0.50 g, 9.3 mmol), *tert*-butyl isocyanide (1.3 mL, 11 mmol) and 5-(trifluoromethyl)pyridin-2-amine (1.51 g, 9.3 mmol), using the general GBB procedure. The reaction mixture was refluxed for 41 hours. The crude product was recrystallized from (MeCN : H_2O) (2 : 1), which furnish the product as beige to orange needles (2.29 g, 72% yield): mp 153-154 °C. R_f = 0.5 (PET : EtOAc) (2 : 1). ^{1}H NMR (400 MHz, Chloroform-*d*) δ 8.61 – 8.55 (m, 1H), 7.64 – 7.56 (m, 2H), 7.36 (dd, *J* = 5.1, 1.1 Hz, 1H), 7.29 – 7.24 (m, 1H), 7.13 (dd, *J* = 5.1, 3.6 Hz, 1H), 3.16 (s, 1H), 1.20 (s, 9H). ^{13}C NMR (151 MHz, Chloroform-*d*) δ 141.85, 136.71, 136.65, 127.57, 125.72, 125.63, 123.99, 123.90 (q, *J* = 270.9 Hz), 122.80 (q, *J* = 5.8 Hz), 120.29 (q, *J* = 2.7 Hz), 117.85, 115.97 (q, *J* = 34.0 Hz), 57.05, 30.63. ^{19}F NMR (376 MHz, Chloroform-*d*) δ -62.08. ESI-MS (m/z) calculated $[M + H]^+$ for $C_{16}H_{17}F_3N_3S$ = 340.11, found 340.1.

***N*-(*tert*-butyl)-6-fluoro-2-(thiophen-2-yl)imidazo[1,2-a]pyridin-3-amine** (**4**). Obtained from 2-thiophenecarboxaldehyde (0.9 mL, 9.3 mmol), NH_4Cl, (0.50 g, 9.4 mmol), *tert*-butyl isocyanide (1.3 mL, 11 mmol, 1.2 equiv.) and 2-amino-5-fluoropyridine (1.04 g, 9.3 mmol), using the general GBB procedure. The reaction mixture was heated for 37 hours. The crude product was recrystallized from (MeCN : H_2O) (1.2 : 1), to furnish the product as beige needles, (1.77 g, 66% yield): mp 188-189 °C. R_f = 0.4 (PET : EtOAc) (2 : 1). ^{1}H NMR (400 MHz, Chloroform-*d*) δ 8.12 (dd, *J* = 4.4, 2.5 Hz, 1H),

7.56 (dd, *J* = 3.6, 1.1 Hz, 1H), 7.49 (dd, *J* = 9.7, 5.0 Hz, 1H), 7.33 (dd, *J* = 5.1, 1.1 Hz, 1H), 7.10 (dd, *J* = 5.1, 3.6 Hz, 1H), 7.04 (ddd, *J* = 10.0, 7.8, 2.5 Hz, 1H), 3.10 (s, 1H), 1.19 (s, 9H). ^{13}C NMR (151 MHz, Chloroform-*d*) δ 153.21 (d, *J* = 236.0 Hz), 139.81, 137.33, 136.48 (d, *J* = 2.3 Hz), 127.47, 125.24, 125.10, 124.30, 117.78 (d, *J* = 8.8 Hz), 116.44 (d, *J* = 25.9 Hz), 110.30 (d, *J* = 41.5 Hz), 56.97, 30.67. ^{19}F NMR (376 MHz, Chloroform-*d*) δ -140.64 (dt, *J* = 8.5, 4.8 Hz). ESI-MS (m/z) calculated $[M + H]^+$ for $C_{15}H_{17}FN_3S$ = 290.11, found 290.1.

***N*-(*tert*-butyl)-6-iodo-2-(thiophen-2-yl)imidazo[1,2-a]pyridin-3-amine** (**5**). Obtained from 2-thiophenecarboxaldehyde (0.4 mL, 4.3 mmol), NH_4Cl, (0.24 g, 4.5 mmol), *tert*-butyl isocyanide (0.8 mL, 7.2 mmol) and 2-amino-5-iodopyridine[45] (1.00 g, 4.5 mmol), using the general GBB procedure. The reaction mixture was refluxed for 6 hours. The crude product was recrystallized from (MeCN : H_2O) (6 : 1), which furnished the product as a white solid (1.18 g, 69% yield): mp 180-181 °C. R_f = 0.7 (PET : EtOAc) (1 : 1). ^{1}H NMR (400 MHz, Chloroform-*d*) δ 8.44 (t, *J* = 1.3 Hz, 1H), 7.59 (d, *J* = 2.6 Hz, 1H), 7.37 – 7.28 (m, 3H), 7.11 (dd, *J* = 5.1, 3.6 Hz, 1H), 3.09 (s, 1H), 1.19 (s, 9H). ^{13}C NMR (151 MHz, Chloroform-*d*) δ 140.73, 137.03, 135.30, 132.30, 128.91, 127.52, 125.43, 125.31, 122.80, 118.37, 74.49, 57.01, 30.70. ESI-MS (m/z) calculated $[M + H]^+$ for $C_{15}H_{17}IN_3S$ = 398.02, found 398.0.

7-bromo-*N*-(*tert*-butyl)-2-(thiophen-2-yl)imidazo[1,2-a]pyridin-3-amine (**6**). Obtained from 2-thiophenecarboxaldehyde (0.4 mL, 4.3 mmol), NH_4Cl, (0.23 g, 4.3 mmol), *tert*-butyl isocyanide (0.60 mL, 5.2 mmol) and 2-amino-4-bromopyridine (0.74 g, 4.3 mmol), using the general GBB procedure. The reaction mixture was refluxed for 38 hours. The crude product was recrystallized from (MeOH : H_2O) (10 : 1) to furnish the product as off-white needles (0.87 g, 52% yield). This product was slightly contaminated with impurities and was used in the subsequent reaction without further purification. mp 172-173 °C. R_f = 0.5 (PET : EtOAc) (2 : 1). ^{1}H NMR (400 MHz, Chloroform-*d*) δ 8.06 (dd, *J* = 7.3, 0.8 Hz, 1H), 7.70 (s, 1H), 7.57 (d, *J* = 3.6 Hz, 1H), 7.33 (dd, *J* = 5.1, 1.1 Hz, 1H), 7.11 (dd, *J* =

5.1, 3.6 Hz, 1H), 6.85 (dd, J = 7.2, 1.9 Hz, 1H), 3.09 (s, 1H), 1.18 (s, 9H). ESI-MS (m/z) calculated $[M + H +]^+$ for $C_{15}H_{16}BrN_3S$ = 350.03, found 350.0 and $[M + H + 2]^+$= 352.1.

General Suzuki-Miyaura cross-coupling procedure:

An aryl halide, such as **1** (1.2 g, 3.4 mmol, 1 equiv.) was dissolved in DME (75 mL) and water (38 mL). A boronic acid, such as phenylboronic acid (0.498 g, 4.1 mmol, 1.2 equiv.), Na_2CO_3 (0.723 g, 6.8 mmol, 2.0 equiv.) and $Pd(PPh_3)_4$ (0.393 g, 0.34 mmol, 10 mol%) were added respectively. The flask was fitted with a rubber septum and purged with argon. The reaction mixture was then heated to reflux until completion of the reaction monitored by HPLC, cooled to room temperature and diluted with water (70 mL) and DCM (100 mL). The aqueous layer was extracted with DCM (100 + 200 mL). The combined organic layers were washed with H_2O (110 mL), dried over Na_2SO_4 and reduced *in vacuo*. The crude product was dissolved in DCM, concentrated onto celite and purified by column chromatography to yield the product and/or purified by recrystallization.

***N*-(*tert*-butyl)-6-phenyl-2-(thiophen-2-yl)imidazo[1,2-*a*]pyridin-3-amine** (**7**). Obtained from **1** (1.2 g, 3.4 mmol) and phenylboronic acid (0.498 g, 4.1 mmol), using the general Suzuki-Miyaura cross-coupling procedure. Purification of the crude product was performed by column chromatography (silica gel 60, 40-63 μM) (DCM : EtOAc) (20 : 1) which furnished the product as a white solid, (0.62 g, 52% yield): mp 147-148°C. R_f = 0.3 (DCM : EtOAc) (20 : 1). R_t = 2.08 min. (4 mL/min flow rate). ^{1}H NMR (400 MHz, Chloroform-*d*) δ 8.38 (dd, J = 1.2 Hz, 1H), 7.63 – 7.54 (m, 4H), 7.53 – 7.44 (m, 2H), 7.43 – 7.37 (m, 2H), 7.32 (dd, J = 5.1, 1.2 Hz, 1H), 7.11 (dd, J = 5.1, 3.6 Hz, 1H), 3.14 (s, 1H), 1.23 (s, 9H).^{13}C NMR (151 MHz, Chloroform-*d*) δ 141.72, 137.96, 137.79, 135.59, 129.25, 127.83, 127.45, 126.97, 125.88, 125.09, 125.02, 124.94, 123.34, 121.02, 117.21, 56.93, 30.79.

***N*-(*tert*-butyl)-2,6-di(thiophen-2-yl)imidazo[1,2-*a*]pyridin-3-amine** (**8**). Obtained from **1** (0.83 g, 2.4 mmol) and 2-thienylboronic acid (0.37 g, 2.9 mmol), using the general Suzuki-Miyaura cross-

coupling procedure. Purification of the crude product was performed by column chromatography (silica gel 60, 40-63 μM) (DCM : MeOH)(40 : 1 MeOH). The product was obtained as an off-white solid. The impure fractions containing the product were combined, reduced *in vacuo* and recrystallized from MeCN and washed with cold MeCN and cold water to yield the product as off-white needles (0.474 g, 60% yield): mp 204-205 °C. R_f = 0.4 (DCM : MeOH)(40 : 1). R_t = 2.39 min (3 mL/min flow rate) (>90% pure by HPLC system 1). ^{1}H NMR (400 MHz, Chloroform-*d*) δ 8.43 (dd, *J* = 1.9, 1.0 Hz, 1H), 7.60 (dd, *J* = 1.0 Hz, 1H), 7.53 (dd, *J* = 9.3, 0.9 Hz, 1H), 7.40 (dd, *J* = 9.3, 1.9 Hz, 1H), 7.32 (ddd, *J* = 7.2, 5.0, 1.1 Hz, 2H), 7.28 (dd, *J* = 3.6, 1.2 Hz, 1H), 7.11 (td, *J* = 3.8 Hz, 2H), 3.13 (s, 1H), 1.23 (s, 9H). ^{13}C NMR (151 MHz, Chloroform-*d*) δ 141.57, 140.85, 137.65, 135.72, 128.33, 127.48, 125.10, 124.99, 124.97, 124.27, 123.73, 123.40, 119.91, 119.89, 117.38, 56.94, 30.81. ESI-MS (m/z) calculated $[M + H]^+$ for $C_{19}H_{20}N_3S_2$ = 354.11, found 354.1.

***6*-bromo-*N*-(*tert*-butyl)-2-cyclopentylimidazo[1,2-*a*]pyridin-3-amine (9).** Obtained from cyclopentanecarbaldehyde (1.0 mL, 9.3 mmol), NH_4Cl, (0.50 g, 9.3 mmol), *tert*-butyl isocyanide (1.3 mL, 11.5 mmol) and 2-amino-5-bromopyridine (1.61 g, 9.3 mmol) using the general GBB procedure. The reaction mixture was refluxed for 46 hours. The crude product was recrystallized from (MeCN : H_2O) (3 : 1), which furnished the product as large, slightly grey crystals (2.10 g, 67% yield): mp 143 °C. R_f = 0.6 (PET : EtOAc) (2 : 1). ^{1}H NMR (400 MHz, Chloroform-*d*) δ 8.26 (dd, *J* = 1.9, 0.8 Hz, 1H), 7.36 (d, *J* = 9.4 Hz, 1H), 7.11 (dd, *J* = 9.4, 2.0 Hz, 1H), 3.23 – 3.11 (m, 1H), 2.75 (s, 1H), 2.00 – 1.90 (m, 6H), 1.76 – 1.63 (m, 2H), 1.21 (s, 9H).^{13}C NMR (101 MHz, Chloroform-*d*) δ 146.08, 140.70, 126.54, 123.59, 123.35, 117.66, 105.68, 55.39, 37.72, 33.92, 30.48, 26.24. ESI-MS (m/z) calculated $[M + H]^+$ for $C_{16}H_{22}BrN$ = 336.1 found 336.1 and $[M + H + 2]^+$ = 338.2.

General *tert*-butyl deprotection procedure:

The *tert*-butyl protected imidazo[1,2-*a*]pyridin-3-amine was suspended in 10-15 mL of 5M aqueous HBr. The reaction mixture was heated to 110 °C until completion monitored by HPLC and/or

TLC, cooled to room temperature and the pH of the reaction mixture adjusted to pH ~ 12-14 via aqueous 5M NaOH. For some compounds, the reaction mixture was cooled by an ice bath during this adjustment of the pH as specified for relevant compounds. The aqueous layer was extracted with EtOAc (3 x 50 mL). The combined organic layers were dried over Na_2SO_4 and subsequently reduced *in vacuo* to yield products as solids. The product was used in the subsequent reaction without further purification unless otherwise specified.

6-bromo-2-(thiophen-2-yl)imidazo[1,2-*a*]pyridin-3-amine (**10**). Obtained from **1** (0.71 g, 2.0 mmol), using the general *tert*-butyl deprotection procedure and was isolated as a yellow crystalline solid (0.58 g, 98% yield): mp 194-195 °C. R_f = 0.5 (Heptane : EtOAc) (3 : 2). R_t = 1.27 min. (4 mL/min flow rate). ^{1}H NMR (400 MHz, Chloroform-*d*) δ 8.16 (dd, *J* = 2.0, 0.9 Hz, 1H), 7.57 (dd, *J* = 3.6, 1.2 Hz, 1H), 7.41 (dd, *J* = 9.4, 0.9 Hz, 1H), 7.35 (dd, *J* = 5.1, 1.1 Hz, 1H), 7.18 – 7.12 (m, 2H), 3.34 (s, 2H). ^{13}C NMR (151 MHz, Chloroform-*d*) δ 139.76, 136.91, 131.33, 127.93, 127.21, 125.17, 124.16, 122.38, 121.63, 117.98, 106.87. ESI-MS (m/z) calculated $[M + H]^+$ for $C_{11}H_9BrN_3S$ = 293.97, found 293.9 and $[M + H + 2]^+$= 295.9.

6-methyl-2-(thiophen-2-yl)imidazo[1,2-*a*]pyridin-3-amine (**11**).[46] Obtained from **2** (0.400 g, 1.4 mmol), using the general *tert*-butyl deprotection procedure. Short reaction time (1.5 hours) adjustment of pH at 0 °C proved vital. The product was isolated as a yellow crystalline solid (0.319 g, 99% yield): mp = 174-175 °C. R_f = 0.3 (Heptane : EtOAc) (1 : 2). R_t = 1.3 min. (4 mL/min flow rate). ^{1}H NMR (400 MHz, Chloroform-*d*) δ 7.79 (t, *J* = 1.6 Hz, 1H), 7.56 (t, *J* = 0.9 Hz, 1H), 7.43 (d, *J* = 9.1 Hz, 1H), 7.31 (dd, *J* = 0.9 Hz, 1H), 7.14 (d, *J* = 3.7 Hz, 1H), 6.96 (d, *J* = 1.6 Hz, 1H), 3.32 (s, 2H), 2.35 (s, 3H). ^{13}C NMR (151 MHz, Chloroform-*d*) δ 140.49, 137.67, 129.92, 127.80, 127.02, 124.48, 123.53, 121.66, 121.32, 119.73, 116.71, 18.52. ESI-MS (m/z) calculated $[M + H]^+$ for $C_{12}H_{11}N_3S$ = 230.7, found 230.5.

2-(thiophen-2-yl)-6-(trifluoromethyl)imidazo[1,2-a]pyridin-3-amine (**12**). Obtained from **3** (0.47 g, 1.4 mmol) using the general *tert*-butyl deprotection procedure. The reaction mixture was cooled on an ice bath upon adjustment of pH with 5M NaOH. The product was isolated as a yellow crystalline solid, (0.329 g, 84% yield): mp 208-209 °C. R_f = 0.7 (Heptane : EtOAc) (1 : 3). R_t = 8.80 min (>95% pure by HPLC system 2). ^{1}H NMR (400 MHz, Chloroform-*d*) δ 8.46 – 8.38 (m, 1H), 7.66 – 7.57 (m, 2H), 7.38 (dd, *J* = 5.1, 1.1 Hz, 1H), 7.29 – 7.23 (m, 1H), 7.16 (dd, *J* = 5.1, 3.6 Hz, 1H), 3.41 (s, 2H). ^{13}C NMR (151 MHz, DMSO-d_6) δ 137.90, 137.72, 128.00, 127.21, 124.53 (q, *J* = 270.9 Hz), 124.27, 123.90, 122.51, 122.13 (q, *J* = 5.9 Hz), 117.16, 116.60 (q, *J* = 2.6 Hz), 113.76 (q, *J* = 33.1 Hz). ^{19}F NMR (376 MHz, DMSO-d_6) δ -60.43. ESI-MS (m/z) calculated $[M+H]^+$ for $C_{12}H_9F_3N_3S$ = 284.05, found 284.0.

6-fluoro-2-(thiophen-2-yl)imidazo[1,2-a]pyridin-3-amine (**13**). Obtained from **4** (0.40 g, 1.4 mmol) using the general *tert*-butyl deprotection procedure. The reaction mixture was cooled on an ice bath upon adjustment of pH with 5M NaOH. The product was isolated as a greenish crystalline solid (0.278 g, 85% yield): mp 201-202 °C (decomp.). R_f = 0.6 (PET : EtOAc) (1 : 3) + 1% Et_3N. ^{1}H NMR (400 MHz, Chloroform-*d*) δ 7.96 – 7.93 (m, 1H), 7.56 (dd, *J* = 3.7, 1.1 Hz, 1H), 7.51 – 7.45 (m, 1H), 7.34 (dd, *J* = 5.1, 1.1 Hz, 1H), 7.14 (dd, *J* = 5.1, 3.6 Hz, 1H), 7.02 (ddd, *J* = 10.1, 8.0, 2.4 Hz, 1H), 3.33 (s, 2H). ^{13}C NMR (151 MHz, Chloroform-*d*) δ 153.52 (d, *J* = 236.4 Hz), 138.95, 137.14, 132.00 (d, *J* = 2.0 Hz), 127.88, 124.96, 123.89, 122.71, 117.83 (d, *J* = 8.9 Hz), 115.76 (d, *J* = 25.9 Hz), 108.74 (d, *J* = 41.4 Hz). ^{19}F NMR (376 MHz, Chloroform-*d*) δ -140.25 (q, *J* = 5.4 Hz). ESI-MS (m/z) calculated $[M+H]^+$ for $C_{11}H_9FN_3S$ = 234.05, found 234.0.

6-iodo-2-(thiophen-2-yl)imidazo[1,2-a]pyridin-3-amine (**14**). Obtained from **5** (0.450 g, 1.1 mmol) using the general *tert*-butyl deprotection procedure. The reaction mixture was cooled on an ice bath upon adjustment of pH with 5M NaOH. The product was isolated as yellow crystalline solid (0.322 g, 83% yield). R_f = 0.7 (Heptane : EtOAc) (1 :3) + 1% Et_3N.^{1}H NMR (400 MHz, Chloroform-

d) δ 8.34 – 8.25 (m, 1H), 7.57 (dd, *J* = 3.6, 1.1 Hz, 1H), 7.35 (dd, *J* = 5.1, 1.1 Hz, 1H), 7.33 – 7.27 (m, 2H), 7.14 (dd, *J* = 5.1, 3.6 Hz, 1H), 3.33 (s, 2H). ^{13}C NMR (151 MHz, DMSO-d_6) δ 138.20, 136.83, 128.88, 127.90, 126.93, 125.53, 123.92, 123.13, 122.12, 117.54, 74.89.ESI-MS (m/z) calculated $[M + H]^+$ for $C_{11}H_9IN_3S$ = 341.96, found 341.9.

7-bromo-2-(thiophen-2-yl)imidazo[1,2-a]pyridin-3-amine (**15**). Obtained from **6** (0.40 g, 1.2 mmol,1 equiv.) using the general *tert*-butyl deprotection procedure. The reaction mixture was cooled by an ice bath upon adjustment of pH with 5M NaOH. The product was isolated as an orange solid (0.313 g, 87% yield). This product was used in the subsequent reactions without further purification. R_f = 0.6 (PET : EtOAc) (1 : 1.5). ^{1}H NMR (400 MHz, Chloroform-*d*) δ 7.91 (d, *J* = 7.2 Hz, 1H), 7.72 (s, 1H), 7.59 (d, *J* = 3.6 Hz, 1H), 7.36 (dd, *J* = 5.1, 1.1 Hz, 1H), 7.15 (dd, *J* = 5.1, 3.6 Hz, 1H), 6.92 (dd, *J* = 7.2, 1.8 Hz, 1H), 3.35 (s, 2H). ESI-MS (m/z) calculated $[M + H]^+$ for $C_{11}H_9BrN_3S$ = 293.97, found 293.9 and $[M + H + 2]^+$= 295.9.

6-phenyl-2-(thiophen-2-yl)imidazo[1,2-*a*]pyridin-3-amine (**16**). Obtained from **7** (0.56 g, 1.6 mmol, 1 equiv.) and 5M aq. HBr (70 mL), using the general *tert*-butyl deprotection procedure,. The product was isolated as a yellow solid (0.435 g, 92% yield): mp 189-191 °C. R_f = 0.7 (PET : EtOAc) (1 : 3). ^{1}H NMR (600 MHz, Chloroform-*d*) δ 8.21 (dd, *J* = 1.9, 1.0 Hz, 1H), 7.64 – 7.57 (m, 4H), 7.48 (dd, *J* = 8.5, 6.9 Hz, 2H), 7.42 – 7.39 (m, 2H), 7.35 (dd, *J* = 5.1, 1.1 Hz, 1H), 7.16 (dd, *J* = 5.1, 3.6 Hz, 1H), 3.39 (s, 2H). ^{13}C NMR (151 MHz, Chloroform-*d*) δ 140.71, 137.76, 137.43, 130.71, 129.22, 127.91, 127.85, 127.00, 126.40, 124.74, 124.55, 123.78, 121.91, 119.36, 117.10. ESI-MS (m/z) calculated $[M + H]^+$ for $C_{17}H_{14}N_3S$ = 292.09, found 292.1.

2,6-di(thiophen-2-yl)imidazo[1,2-*a*]pyridin-3-amine (**17**). Obtained from **8** (0.110 g, 0.30 mmol 1 equiv.) using the general *tert*-butyl deprotection procedure, 5M aq. HBr (26 mL) and was isolated as a yellow crystalline solid (0.087 g, 94% yield): mp 197-198 °C. R_f = 0.6 (PET : EtOAc) (1 : 3). R_t = 1.95 min (3 mL/min).^{1}H NMR (400 MHz, Chloroform-*d*) δ 8.23 (dd, *J* = 1.8, 1.0 Hz, 1H), 7.59

(dd, *J* = 3.6, 1.0 Hz, 1H), 7.54 (dd, *J* = 9.3, 1.0 Hz, 1H), 7.38 (dd, *J* = 9.3, 1.9 Hz, 1H), 7.35 – 7.29 (m, 3H), 7.15 (dd, *J* = 5.1, 3.6 Hz, 1H), 7.12 (dd, *J* = 5.1, 3.6 Hz, 1H), 3.38 (s, 2H). ^{13}C NMR (151 MHz, Chloroform-*d*) δ 140.62, 140.58, 137.33, 130.93, 128.30, 127.87, 125.10, 124.83, 123.88, 123.84, 123.75, 121.93, 120.40, 118.16, 117.28. ESI-MS (m/z) calculated $[M+H]^+$ for $C_{15}H_{11}N_3S_2$ = 298.05, found 298.0.

6-bromo-2-cyclopentylimidazo[1,2-*a*]pyridin-3-amine (**18**). Obtained from **9** (0.242 g, 0.7 mmol, 1 equiv.) using the general *tert*-butyl deprotection procedure. The extraction was performed with EtOAc (2 x 200 mL) and once with a mixture of MeOH (30 mL) in EtOAc (200 mL) to obtain complete extraction of the product. The compound was isolated as an orange solid (0.196 g, 100% yield). R_f = 0.5 (Heptane : EtOAc) (1 : 3) + 1% Et_3N. R_t = 1.57 (3 mL/min flow rate). ^{1}H NMR (400 MHz, Chloroform-*d*) δ 8.14 (dd, *J* = 2.0, 0.9 Hz, 1H), 7.37 (dd, *J* = 9.4, 0.9 Hz, 1H), 7.09 (dd, *J* = 9.5, 1.9 Hz, 1H), 3.28 – 3.16 (m, 1H), 3.00 (s, 2H), 2.07 – 2.00 (m, 2H), 1.96 – 1.81 (m, 4H), 1.75 – 1.66 (m, 2H). ^{13}C NMR (101 MHz, Chloroform-*d*) δ 141.41, 139.35, 125.75, 122.13, 121.80, 117.65, 106.19, 37.72, 33.04, 25.99. ESI-MS (m/z) calculated $[M+H]^+$ for $C_{12}H_{14}BrN_3$ = 280.04, found 280.0 and $[M+H+2]^+$ = 282.0.

3-nitro-2-phenylimidazo[1,2-*a*]pyridine (**22**).[47] Obtained from **21**[35] (0.500 g, 2.5 mmol), phenyl boronic acid (0.370 g, 3.0 mmol), Na_2CO_3 (0.268 g, 2.5 mmol, 1 equiv.) and $Pd(PPh_3)_4$ (0.288 g, 0.25 mmol, 10 mol%) using the general Suzuki-Miyaura cross-coupling procedure. The crude product was dissolved in DCM, concentrated onto silica gel 60 (40-63 μm) and subsequently purified by column chromatography (EtOAc : Heptane) (1 : 1) to furnish the product as a yellow solid (0.525 g, 88% yield). ^{1}H NMR (400 MHz, Chloroform-*d*) δ 9.52 (dt, *J* = 7.1, 1.2 Hz, 1H), 7.96 – 7.87 (m, 2H), 7.85 (dt, *J* = 8.9, 1.1 Hz, 1H), 7.66 (ddd, *J* = 8.9, 7.0, 1.3 Hz, 1H), 7.57 – 7.47 (m, 3H), 7.29 (td, *J* = 7.0, 1.3 Hz, 1H). ^{13}C NMR (151 MHz, Chloroform-*d*) δ 150.42, 145.29, 132.02, 130.98, 130.33, 130.18,

129.10, 128.32, 128.28, 118.46, 116.61. The spectral data was consistent with previous reported data.[47]

2-phenylimidazo[1,2-*a*]pyridin-3-amine (**23**).[34] **22** (1.00 g, 4.2 mmol) was dissolved in MeOH (39 mL) and then $SnCl_2$ (3.98 g, 20.0 mmol) was added. The reaction was stirred overnight at reflux (65 °C). The reaction mixture was then cooled to room temperature and the solvent was removed *in vacuo*. A small amount of EtOAc was then added and the pH of the solution was adjusted with 5M aqueous NaOH to pH~7. The reaction was let stirring for 2 hours. Additional EtOAc was added and the solution was filtered through celite. The compound was then extracted through continuous extraction overnight using EtOAc and reduced *in vacuo* to obtain the product as a white solid (0.740 g, 83% yield). ^{1}H NMR (400 MHz, Chloroform-*d*) δ 8.04 – 7.94 (m, 3H), 7.55 (dt, *J* = 9.1, 1.1 Hz, 1H), 7.47 (dd, *J* = 8.4, 7.0 Hz, 2H), 7.37 – 7.28 (m, 1H), 7.11 (ddd, *J* = 9.1, 6.7, 1.3 Hz, 1H), 6.81 (td, *J* = 6.7, 1.1 Hz, 1H), 3.40 (s, 2H).^{13}C NMR (151 MHz, Methanol-d_4) δ 141.62, 135.56, 130.66, 129.60, 128.16, 127.91, 126.69, 124.67, 123.53, 116.95, 112.92. The spectral data in Chloroform-*d* was consistent with previous reported data.[34]

General acylation procedure for the synthesis of imidazo[1,2-a]pyridine benzamides:

Flame or oven dried glassware was used. The imidazo[1,2-*a*]pyridine-3-amines (0.5 mmol, 1 equiv.) were suspended in dry toluene (3 mL) and dry pyridine (1 mL). The flask was fitted with a rubber septum and purged with argon. The acyl chloride (1.2 equiv.) was added at once through the septum and the reaction mixture was stirred at room temperature monitored by TLC, UPLC-ESI-MS and/or HPLC. The crude product was obtained and purified as specified.

***N*-(6-bromo-2-(thiophen-2-yl)imidazo[1,2-*a*]pyridin-3-yl)benzamide** (**24**). Obtained from **10** (0.145 g, 0.5 mmol) and benzoyl chloride (0.07 mL, 0.6 mmol) using the general acylation procedure for imidazo[1,2-*a*]pyridine benzamides. The crude product was obtained by adding 1.5 mL of water to the reaction mixture, which was subsequently stirred for 30 minutes. The reaction mixture was

cooled on an ice bath and the precipitate was collected by filtration and washed with cold water (5 °C, 3 x 3 mL) and cold acetone (-18 °C, 3 mL) to yield the crude product. The crude product was recrystallized from toluene, which furnished the product as a white solid: mp 269 °C. R_f = 0.4 (DCM : EtOAc) (5 : 1). R_t = 1.58 min (4 mL/min flow rate) (>95% pure by HPLC system 1). ^{1}H NMR (400 MHz, Methanol-d_4) δ 8.27 (t, J = 1.3 Hz, 1H), 8.19 – 8.12 (m, 2H), 7.74 – 7.65 (m, 1H), 7.65 – 7.57 (m, 3H), 7.55 – 7.45 (m, 3H), 7.13 (dd, J = 5.1, 3.7 Hz, 1H). ^{13}C NMR (151 MHz, Methanol-d_4) δ 170.17, 142.95, 136.78, 135.80, 134.03, 134.00, 130.84, 129.97, 129.27, 128.69, 127.56, 126.73, 124.85, 118.23, 115.98, 108.66. ESI-MS (m/z) calculated $[M + H]^+$ for $C_{18}H_{12}BrN_3OS$ = 398.00, found 398.5 and $[M + H + 2]^+$ = 400.5.

***N*-(6-bromo-2-(thiophen-2-yl)imidazo[1,2-*a*]pyridin-3-yl)-4-phenoxybenzamide** (**25**). Obtained from **10** (0.140 g, 0.50 mmol) and 4-phenoxybenzoyl chloride (0.140 g, 0.6 mmol) using the general acylation procedure for imidazo[1,2-a]pyridine benzamides. The reaction mixture was reduced *in vacuo* and the resulting solid washed with cold H_2O, cold acetone and dried *in vacuo*. The product was purified by trituration from MeOH and subsequently washed with H_2O and MeOH and dried under high vacuum. The product was isolated as a white solid (0.047 g, 20% yield): mp 266 °C. R_f = 0.6 (PET : EtOAc) (1 : 2) + 1% Et_3N. R_t = 2.35 min (3 mL/min flow rate) (>99% pure by HPLC system 1). ^{1}H NMR (400 MHz, DMSO-d_6) δ 10.59 (s, 1H), 8.53 (d, J = 2.3 Hz, 1H), 8.21 – 8.13 (m, 2H), 7.64 – 7.54 (m, 2H), 7.51 – 7.42 (m, 4H), 7.28 – 7.23 (m, 1H), 7.22 – 7.10 (m, 5H). ^{13}C NMR (151 MHz, DMSO-d_6) δ 165.89, 160.50, 155.39, 140.52, 135.67, 134.80, 130.55, 130.33, 128.45, 127.92, 127.52, 126.55, 124.78, 124.55, 123.94, 119.72, 117.68, 117.44, 115.03, 106.48. ESI-MS (m/z) calculated $[M + H]^+$ for $C_{24}H_{16}BrN_3O_2S$ = 490.0, found 490.0 and $[M + H + 2]^+$ = 492.0.

***N*-(6-bromo-2-cyclopentylimidazo[1,2-*a*]pyridin-3-yl)benzamide** (**26**). Obtained from **18** (0.223 g, 0.8 mmol) and benzoyl chloride (0.1 mL, 1.1 mmol) using the general acylation procedure for imidazo[1,2-a]pyridine benzamides. No precipitate formed upon addition of 1.5 mL of water to

the reaction mixture. The reaction mixture was reduced *in vacuo* and then concentrated on celite and purified by column chromatography (silica gel 60, 40-63 μM) (DCM : MeOH : Et_3N) (20 : 0.5 : 0.01). Selected pure fraction were combined and reduced and the resulting product was then triturated from MeCN, reduced *in vacuo,* then under high vacuum and finally lyophilized to yield the product as a white solid (0.012 g, 4% yield). R_f = 0.5 (DCM : MeOH) (40 : 1) + 1% Et_3N. R_t = 10.40 min (>99% pure by HPLC system 2). ^{1}H NMR (400 MHz, DMSO-d_6) δ 10.30 (s, 1H), 8.35 (d, *J* = 1.9 Hz, 1H), 8.11 – 8.04 (m, 2H), 7.70 – 7.61 (m, 1H), 7.57 (dd, *J* = 8.4, 6.8 Hz, 2H), 7.52 (d, *J* = 9.5 Hz, 1H), 7.34 (dd, *J* = 9.5, 1.9 Hz, 1H), 3.14 (p, *J* = 8.1 Hz, 1H), 1.94 (dtd, *J* = 10.7, 6.6, 5.2, 2.7 Hz, 2H), 1.83 – 1.71 (m, 4H), 1.60 (dt, *J* = 8.6, 4.7 Hz, 2H). ^{13}C NMR (151 MHz, DMSO-d_6) δ 166.51, 145.55, 139.96, 133.12, 132.12, 128.45, 128.08, 126.61, 123.41, 117.58, 115.66, 105.51, 37.06, 32.28, 25.34. ESI-MS (m/z) calculated $[M + H]^+$ for $C_{19}H_{18}BrN_3O$ = 384.07, found 384.1 and $[M + H + 2]^+$ = 386.0.

***N*-(6-phenyl-2-(thiophen-2-yl)imidazo[1,2-*a*]pyridin-3-yl)benzamide** (**27**). Obtained from **16** (0.150 g, 0.5 mmol) and benzoyl chloride (0.07 mL, 0.6 mmol) using the general acylation procedure for imidazo[1,2-a]pyridine benzamides. The reaction mixture was reduced *in vacuo* and the resulting solid was recrystallized from THF to yield the product as a white solid (0.034 g, 17% yield): mp 270-271°C. R_f = 0.4 (PET : EtOAc) (1 : 3). R_t = 11.37 min. (>95% pure by HPLC system 2). ^{1}H NMR (600 MHz, Methanol-d_4) δ 8.76 (t, *J* = 1.4 Hz, 1H), 8.36 (dd, *J* = 9.3, 1.7 Hz, 1H), 8.19 (d, *J* = 7.4 Hz, 2H), 8.04 (d, *J* = 1.0 Hz, 1H), 7.80 (ddd, *J* = 12.5, 4.4, 1.1 Hz, 2H), 7.76 – 7.70 (m, 3H), 7.64 (t, *J* = 7.8 Hz, 2H), 7.54 (dd, *J* = 8.3, 6.6 Hz, 2H), 7.52 – 7.45 (m, 1H), 7.29 (t, *J* = 3.9 Hz, 1H). ^{13}C NMR (151 MHz, Methanol-d_4) δ 170.42, 139.02, 136.17, 135.73, 134.46, 133.58, 133.39, 131.42, 130.54, 130.40, 130.05, 129.74, 129.53, 129.30, 128.65, 128.55, 127.71, 123.58, 117.88, 113.17. ESI-MS (m/z) calculated $[M + H]^+$ for $C_{24}H_{17}N_3OS$ =396.12, found 396.2 and 397.2.

***N*-(2,6-di(thiophen-2-yl)imidazo[1,2-*a*]pyridin-3-yl)benzamide** (**28**). Obtained from **17** (0.23 g, 0.9 mmol) and benzoyl chloride (0.1 mL 1.0 mmol) using the general acylation procedure for imidazo[1,2-a]pyridine benzamides. The crude product was obtained by adding 0.5 mL of water to the reaction mixture and stirred for 30 minutes. The reaction mixture was cooled by an ice bath and the precipitate was collected by filtration and washed with cold water to yield the crude product (0.247 g). 0.125 g of the crude product was recrystallized from EtOH, then dried *in vacuo* and finally dried under high vacuum. The product was isolated as a white solid (0.038 g, 32% yield): mp 253 °C. R_f = 0.3 (DCM : MeOH) (40 : 1) + 1% Et_3N. R_t = 11.27 min (>99% pure by HPLC system 2). ^{1}H NMR (400 MHz, DMSO-d_6) δ 10.67 (s, 1H), 8.35 (d, *J* = 1.6 Hz, 1H), 8.20 – 8.13 (m, 2H), 7.75 – 7.55 (m, 8H), 7.51 (d, *J* = 3.6 Hz, 1H), 7.15 (ddd, *J* = 8.6, 5.1, 3.6 Hz, 2H). ^{13}C NMR (151 MHz, DMSO-d_6) δ 166.70, 141.27, 139.14, 136.08, 134.80, 133.04, 132.38, 128.66, 128.50, 128.13, 127.88, 126.29, 126.02, 124.90, 124.76, 124.52, 119.97, 118.98, 117.06, 115.01. ESI-MS (m/z) calculated $[M + H]^+$ for $C_{22}H_{15}N_3OS_2$ = 402.07, found 402.1.

***N*-(2-phenylimidazo[1,2-*a*]pyridin-3-yl)benzamide** (**29**).[48] Benzoyl chloride (0.141 g, 1.0 mmol) in DCM (0.7 mL) was slowly added to stirring solution of DIPEA (0.174 g, 1.35 mmol) and **23** (0.15 g, 0.7 mmol) in DCM at 0°C. The reaction was let stirring for 3 hours at room temperature, monitored by TLC. The reaction mixture was reduced *in vacuo* and the resulting product was purified by column chromatography (EtOAc : Heptane) (6 : 4) + 1% Et_3N to furnish the product as a white solid (0.117 g, 52% yield): mp 214-215 °C. R_t = 1.77 min (94% pure by HPLC system 1). ^{1}H NMR (600 MHz, DMSO-d_6) δ 10.71 (s, 1H), 8.12 (ddt, *J* = 8.2, 6.9, 1.2 Hz, 3H), 8.03 – 7.91 (m, 2H), 7.77 – 7.59 (m, 4H), 7.51 – 7.40 (m, 2H), 7.37 – 7.30 (m, 2H), 6.96 (td, *J* = 6.7, 1.1 Hz, 1H).^{13}C NMR (151 MHz, DMSO-d_6) δ 166.70, 142.08, 137.83, 133.59, 132.98, 132.36, 128.68, 128.55, 128.00, 127.68, 126.63, 125.20, 123.77, 116.92, 115.44, 112.24. ESI-MS (m/z) calculated $[M + H]^+$ for $C_{20}H_{16}N_3O$ = 314.13, found 314.1.

4-chloro-*N*-(6-methyl-2-(thiophen-2-yl)imidazo[1,2-*a*]pyridin-3-yl)benzamide (**30**). Obtained from **11** (0.130 g, 0.57 mmol) and 4-chlorobenzoyl chloride (0.090 mL 0.70 mmol, 1.2 equiv.) using the general acylation procedure for imidazo[1,2-a]pyridine benzamides. The crude product was obtained by adding 0.9 mL of distilled water to the reaction mixture and stirred at 0 °C for 30 minutes. The precipitating white solid was collected by filtration and washed with water and recrystallized from EtOAc. Filtration and dried *in vacuo* and freeze dried furnished the product as a white crystalline solid (0.095 g, 46% yield): mp = 276 °C. R_f = 0.2 (Heptane : EtOAc) (1 : 2) + 1% Et_3N. R_t = 10.61 min (>98% pure by HPLC system 2). ^{1}H NMR (400 MHz, DMSO-d_6) δ 10.67 (s, 1H), 8.19 – 8.12 (m, 2H), 8.03 – 7.98 (m, 1H), 7.74 – 7.66 (m, 2H), 7.53 (dt, *J* = 6.8, 1.6 Hz, 2H), 7.45 (dd, *J* = 3.7, 1.2 Hz, 1H), 7.21 (dd, *J* = 9.2, 1.7 Hz, 1H), 7.11 (dd, *J* = 5.1, 3.6 Hz, 1H), 2.30 (s, 3H). ^{13}C NMR (151 MHz, DMSO-d_6) δ 165.67, 141.12, 137.25, 136.26, 133.84, 131.80, 130.01, 128.74, 128.56, 127.79, 125.94, 124.15, 121.91, 121.19, 115.97, 113.82, 17.52. ESI m/z calculated $[M+H]^+$ for $C_{19}H_{15}ClN_3OS$ = 368.06, found 368.1 and $[M+H+2]^+$ 370.1.

4-chloro-*N*-(2-(thiophen-2-yl)-6-(trifluoromethyl)imidazo[1,2-a]pyridin-3-yl)benzamide (**31**). Obtained from **12** (0.166 g, 0.59 mmol) and 4-chlorobenzoyl chloride (0.090 mL 0.70 mmol) using the general acylation procedure for imidazo[1,2-a]pyridine benzamides. The crude product was obtained by adding 1 mL of water to the reaction mixture and stirred at 0 °C for 30 minutes. The precipitating solid was collected by filtration and washed with water and then dried *in vacuo*. To the filtrate was added water (15 mL) and this aqueous layer was extracted with DCM (2 x 15 mL). The combined organic layers were dried over Na_2SO_4, combined with the initially collected precipitate and reduced *in vacuo* to furnish the crude product. The crude product was concentrated on celite and purified by column chromatography (silica gel 60, 40-63 μM) (Heptane : EtOAc) (1 : 0.9), reduced under high vacuum and freeze dried. The product was isolated as a white solid (0.034 g, 14% yield): mp 268 °C. R_f = 0.4 (Heptane : EtOAc) (1 : 0.9). R_t = 12.89 min (>99% pure by HPLC system 2).^{1}H

NMR (400 MHz, DMSO-d_6) δ 10.79 (s, 1H), 8.93 – 8.82 (m, 1H), 8.23 – 8.09 (m, 2H), 7.83 (d, J = 9.4 Hz, 1H), 7.75 – 7.68 (m, 2H), 7.63 – 7.56 (m, 2H), 7.54 (dd, J = 3.6, 1.2 Hz, 1H), 7.15 (dd, J = 5.1, 3.6 Hz, 1H). ^{13}C NMR (151 MHz, DMSO-d_6) δ 165.81, 141.92, 137.29, 135.84, 135.26, 131.77, 130.18, 128.66, 128.01, 127.03, 125.31, 123.87 (q, J = 5.5 Hz), 121.14 (q, J = 271.3 Hz), 120.90 (q, J = 3.3, 2.0 Hz), 117.66, 115.83, 115.07 (q, J = 33.6 Hz). ^{19}F NMR (376 MHz, DMSO-d_6) δ -59.90. ESI m/z calculated $[M+H]^+$ for $C_{19}H_{12}ClF_3N_3OS$ = 422.03, found 422.1 and $[M+H+2]^+$= 424.1.

4-chloro-N-(6-fluoro-2-(thiophen-2-yl)imidazo[1,2-a]pyridin-3-yl)benzamide (**32**). Obtained from **13** (0.210 g, 0.9 mmol) and 4-chlorobenzoyl chloride (0.1 mL 0.8 mmol) using the general acylation procedure for imidazo[1,2-a]pyridine benzamides. The crude product was obtained by adding 1.5 mL of water to the reaction mixture and stirred at 0 °C for 30 minutes. The precipitating solid was collected by filtration and washed with water and dried *in vacuo* to yield the crude product. The crude product was triturated from EtOAc(15 mL), purified by recrystallizations, first from EtOAc (15 mL) and then from MeOH (14 mL), and dried *in vacuo* to furnish the product as a white solid (0.052g, 16% yield): mp 289 °C. R_f = 0.4 (PET : EtOAc) (2 : 1). R_t = 10.73 min (>99% pure by HPLC system 2). ^{1}H NMR (400 MHz, DMSO-d_6) δ 10.73 (s, 1H), 8.51 (dd, J = 4.5, 2.4 Hz, 1H), 8.18 – 8.11 (m, 2H), 7.73 – 7.65 (m, 3H), 7.56 (dd, J = 5.1, 1.2 Hz, 1H), 7.48 (dd, J = 3.7, 1.2 Hz, 1H), 7.42 (ddd, J = 10.1, 8.3, 2.5 Hz, 1H), 7.13 (dd, J = 5.1, 3.6 Hz, 1H). ^{13}C NMR (151 MHz, DMSO-d_6) δ 165.66, 152.88 (d, J = 233.8 Hz), 139.86, 137.22, 135.90, 135.46 (d, J = 2.1 Hz), 131.82, 130.10, 128.66, 127.89, 126.32, 124.53, 117.47 (d, J = 9.1 Hz), 117.14 (d, J = 25.8 Hz), 115.71 (d, J = 1.9 Hz), 111.09 (d, J = 41.8 Hz). ^{19}F NMR (376 MHz, DMSO-d_6) δ -140.31 (dt, J = 9.2, 4.8 Hz). ESI m/z calculated $[M+H]^+$ for $C_{18}H_{12}ClFN_3OS$ = 372.04, found 372.0 and $[M+H+2]^+$ = 374.1.

4-chloro-*N*-(6-iodo-2-(thiophen-2-yl)imidazo[1,2-a]pyridin-3-yl)benzamide (**33**)**.** Obtained from **14** (0.272 g, 0.8 mmol) and 4-chloro benzoyl chloride (0.159 g, 0.9 mmol) using the general acylation procedure for imidazo[1,2-a]pyridine benzamides. The crude product was obtained by

adding water (1.5 mL) to the reaction mixture and which was then cooled by an ice bath for 30 minutes. The precipitate was collected by filtration, washed with water and dried *in vacuo* to yield the crude product. Recrystallization from MeOH (26 mL) and drying *in vacuo* furnish the product as white needles (0.087 g, 23% yield): mp 279-280 °C. R_f = 0.5 (Heptane : EtOAc) (1 : 2). R_t = 11.55 min (>99% pure by HPLC system 2). ^{1}H NMR (400 MHz, DMSO-d_6) δ 10.68 (s, 1H), 8.59 (d, J = 1.5 Hz, 1H), 8.18 – 8.10 (m, 2H), 7.70 (d, J = 8.5 Hz, 2H), 7.59 – 7.50 (m, 2H), 7.50 – 7.42 (m, 2H), 7.12 (dd, J = 5.1, 3.6 Hz, 1H). ^{13}C NMR (151 MHz, DMSO-d_6) δ 165.75, 140.74, 137.22, 135.66, 134.36, 133.12, 131.81, 130.13, 128.64, 128.37, 127.90, 126.49, 124.73, 117.88, 114.06, 76.49. ESI m/z calculated $[M+H]^+$ for $C_{18}H_{11}ClIN_3OS$ = 479.94, found 480.0 and $[M+H+2]^+$ = 482.0.

***N*-(7-bromo-2-(thiophen-2-yl)imidazo[1,2-a]pyridin-3-yl)-4-chlorobenzamide** (**34**). Obtained from **15** (0.216 g, 0.7 mmol) and 4-chlorobenzoyl chloride (0.129 g, 0.7 mmol) using the general acylation procedure for imidazo[1,2-a]pyridine benzamides. The crude product was obtained by adding water (2 mL) to the reaction mixture, which was then cooled on an ice bath for 30 minutes. The precipitate was collected by filtration, washed with water and dried *in vacuo* to yield the crude product. Recrystallization from MeOH (14 mL), drying *in vacuo* with Et_2O (5 mL) added twice which furnished the product as white needles (0.071g, 23% yield): mp 266 °C. R_f = 0.6 (Heptane: EtOAc) (1 : 1). R_t = 11.41 min (>95% pure by HPLC system 2). ^{1}H NMR (400 MHz, DMSO-d_6) δ 10.77 (s, 1H), 8.18 (d, J = 7.2 Hz, 1H), 8.14 (d, J = 8.6 Hz, 2H), 7.96 (d, J = 1.8 Hz, 1H), 7.75 – 7.65 (m, 2H), 7.58 (dd, J = 5.1, 1.2 Hz, 1H), 7.50 (dd, J = 3.6, 1.2 Hz, 1H), 7.19 – 7.08 (m, 2H). ^{13}C NMR (151 MHz, DMSO-d_6) δ 165.68, 142.21, 137.34, 135.60, 134.69, 131.63, 130.02, 128.76, 127.94, 126.58, 125.00, 124.83, 118.57, 118.51, 115.76, 114.62. ESI m/z calculated $[M+H]^+$ for $C_{18}H_{12}BrClN_3OS$ = 431.96, found 432.0 and $[M+H+2]^+$= 434.0.

3-bromo-2-phenylimidazo[1,2-a]pyridine (**37**).[51] 2-phenylimidazo[1,2-a]pyridine[49,50] (0.822 g, 4.2 mmol) was dissolved in MeCN (25 mL) and NBS (0.839 g, 4.7 mmol) was added at once. The

reaction mixture was stirred at room temperature in the dark until completion by TLC (1.5 hours). The reaction mixture was reduced *in vacuo* and the residue was taken up in DCM (150 mL). The organic layer was washed with 2 M NaOH (80 mL), with a sat. $Na_2S_2O_3$ (100 mL) and H_2O (80 mL). The organic layer was dried over $MgSO_4$ and reduced *in vacuo* to yield the product as a dark oil, which solidified over time to glossy dark crystals (1.13 g, 98% yield). This product was used in the subsequent reactions without further purification. R_f = 0.5 (Heptane : EtOAc) (1 : 1) + 1% Et_3N. ^{1}H NMR (400 MHz, Chloroform-*d*) δ 8.19 (dt, *J* = 7.0, 1.1 Hz, 1H), 8.17 – 8.11 (m, 2H), 7.65 (dt, *J* = 9.0, 1.1 Hz, 1H), 7.52 – 7.46 (m, 2H), 7.42 – 7.36 (m, 1H), 7.29 – 7.22 (m, 1H), 6.94 (td, *J* = 6.8, 1.1 Hz, 1H). ^{13}C NMR (151 MHz, Chloroform-*d*) δ 145.61, 142.85, 133.02, 128.61, 128.44, 128.04, 125.22, 124.11, 117.79, 113.19, 91.85. The spectral data was consistent with previous reported data.[52, 53] ESI-MS (m/z) calculated $[M + H]^+$ for $C_{13}H_9BrN_2$ = 273.00, found 273.0 and $[M + H + 2]^+$ = 275.0.

3-iodo-2-phenylimidazo[1,2-a]pyridine (**38**)[54] Obtained via a procedure similar to the synthesis of **37**, from 2-phenylimidazo[1,2-a]pyridine (0.860 g, 4.4 mmol) and *N*-iodosuccinimide (1.15 g, 5.4 mmol.). Also, this reaction was conducted under argon. The product was isolated as a pale brown solid, 1.22 g, 3.8 mmol, 85% yield. This product was used in the subsequent reactions without further purification. R_f = 0.4 (Heptane : EtOAc) (1 : 1) + 1 % Et_3N. ^{1}H NMR (400 MHz, Chloroform-*d*) δ 8.24 (dt, *J* = 6.9, 1.2 Hz, 1H), 8.09 – 8.03 (m, 2H), 7.63 (dt, *J* = 9.0, 1.1 Hz, 1H), 7.53 – 7.44 (m, 2H), 7.43 – 7.37 (m, 1H), 7.27 (ddd, *J* = 9.0, 6.8, 1.3 Hz, 1H), 6.94 (td, *J* = 6.8, 1.2 Hz, 1H). ^{13}C NMR (151 MHz, Chloroform-*d*) δ 148.29, 148.25, 133.73, 128.66, 128.49, 128.47, 126.66, 125.66, 117.76, 113.29, 59.57. The spectral data was consistent with previous reported data.[55, 56] ESI-MS (m/z) calculated $[M + H]^+$ for $C_{13}H_{10}IN_2$ = 320.99, found 320.9.

2-phenyl-3-((trimethylsilyl)ethynyl)imidazo[1,2-a]pyridine (**39**). This compound was synthesized from **37** (0.400 g, 1.5 mmol), which was placed in a microwave tube. CuI, (0.043 g, 0.23

mmol, 15 mol%), $Pd(PPh_3)_2Cl_2$ (0.154 g, 0.22 mmol, 15 mol%) were added. The tube was sealed and purged with argon. Ethynyltrimethylsilane (0.25 mL, 1.8 mmol) and triethylamine (4.5 mL) were added. The reaction mixture was heated to 80 °C until completion by TLC (23 hours) and cooled to room temperature. The reaction mixture was diluted with water (30 mL) and Et_2O (100 mL). The aqueous layer was extracted with Et_2O (2 x 80 mL). The combined organic layers were dried over Na_2SO_4 and reduced *in vacuo*. The crude product was concentrated on celite and purified by column chromatography (silica gel 60, 40-63 μM) (PET : EtOAc) (3 : 1). The product was isolated as a pale yellow solid (0.211 g, 50% yield). R_f = 0.3 (PET : EtOAc) (3 : 1). ^{1}H NMR (400 MHz, Chloroform-*d*) δ 8.39 – 8.32 (m, 2H), 8.29 (dt, *J* = 6.8, 1.2 Hz, 1H), 7.65 (dt, *J* = 8.9, 1.1 Hz, 1H), 7.50 – 7.42 (m, 2H), 7.41 – 7.34 (m, 1H), 7.32 – 7.27 (m, 1H), 6.93 (td, *J* = 6.8, 1.1 Hz, 1H), 0.35 (s, 9H). ^{13}C NMR (151 MHz, Chloroform-*d*) δ 148.65, 145.16, 133.53, 128.71, 128.56, 127.37, 126.46, 125.47, 117.60, 113.07, 108.17, 105.04, 93.83, 0.07.

2-phenyl-3-(1-phenyl-1H-1,2,3-triazol-4-yl)imidazo[1,2-a]pyridine (**40**). A flask was charged with previously lyophilized **39** (0.200 g, 0.69 mmol) and TBAF (0.345 g, 1.3 mmol). The flask was fitted with a rubber septum and purged with argon. Then, dry THF (10 mL) was added through the septum. The reaction mixture was stirred at room temperature until completion by TLC (1.5 hours). The reaction mixture was reduced *in vacuo* and the residue was taken up in a 10% aqueous solution of NH_4Cl (20 mL) and DCM (20 mL). The aqueous layer was extracted with DCM (2 x 20 mL) and the combined organic layers dried over Na_2SO_4 and reduced *in vacuo* to yield the crude product. The crude product was concentrated on celite and purified by column chromatography (silica gel 60, 40-63 μM) (PET : EtOAc) (2 : 1) to furnish 3-ethynyl-2-phenylimidazo[1,2-a]pyridine as a white solid (0.123 g, 82% yield): mp 141-142 °C (decomp). R_f = 0.4 (PET : EtOAc) (2 : 1). ^{1}H NMR (400 MHz, Chloroform-*d*) δ 8.36 – 8.28 (m, 3H), 7.67 (dt, *J* = 9.1, 1.1 Hz, 1H), 7.51 – 7.45 (m, 2H), 7.42 – 7.36 (m, 1H), 7.30 (ddd, *J* = 9.1, 6.8, 1.3 Hz, 1H), 6.94 (td, *J* = 6.8, 1.2 Hz, 1H), 4.07 (s, 1H). ^{13}C NMR

(151 MHz, Chloroform-*d*) δ 149.11, 145.41, 133.41, 128.92, 128.76, 127.46, 126.64, 125.39, 117.74, 113.27, 103.96, 90.04, 73.45. A flask was charged with 3-ethynyl-2-phenylimidazo[1,2-a]pyridine (0.114 g, 0.52 mmol), $CuSO_4 \cdot 5H_2O$ (0.0261g, 0.10 mmol, 20 mol%) and (+)-Sodium L-ascorbate (0.0534 g, 0.27 mmol, 51 mol%). The flask was fitted with a rubber septum and purged with argon. THF (15 mL), H_2O (10 mL) and 1.0 mL of a ~0.5M solution of azidobenzene in *tert*-butyl methyl ether (~0.52 mmol) was then added through the septum. The reaction mixture was stirred at room temperature, in the dark, monitored by TLC (17.5 hours). The reaction mixture was poured into H_2O (100 mL) and EtOAc (100 mL). The aqueous layer was extracted with EtOAc (2 x 100 mL). The combined organic layers were dried over Na_2SO_4 and then reduced *in vacuo*. The crude product was concentrated on celite and purified by column chromatography (40-63 μm silica gel 60) (PET : EtOAc) (1 : 1) to yield the product as a white solid (0.137 g, 78% yield): mp 188-189 °C. R_f = 0.6 (PET : EtOAc) (1 : 2). R_t = 10.62 min (>99% pure by HPLC system 2). ^{1}H NMR (400 MHz, DMSO-d_6) δ 9.19 (s, 1H), 8.46 (dd, *J* = 6.9, 1.2 Hz, 1H), 8.05 – 7.97 (m, 2H), 7.85 – 7.78 (m, 2H), 7.75 – 7.71 (m, 1H), 7.65 (dd, *J* = 8.6, 7.1 Hz, 2H), 7.59 – 7.51 (m, 1H), 7.45 – 7.37 (m, 3H), 7.36 – 7.29 (m, 1H), 7.00 (td, *J* = 6.8, 1.2 Hz, 1H). ^{13}C NMR (151 MHz, DMSO-d_6) δ 144.79, 143.86, 136.85, 136.48, 133.88, 129.93, 128.96, 128.43, 127.95, 127.76, 125.97, 125.21, 123.81, 120.23, 116.87, 112.97, 110.71. ESI-MS (m/z) calculated $[M + H]^+$ for $C_{21}H_{16}N_5$ = 338.1, found 338.1.

3-(4-chlorophenyl)-5-(2-phenylimidazo[1,2-a]pyridin-3-yl)-1,2,4-oxadiazole (42) 41[39] (0.171 g, 0.64 mmol) and 4-chloro-N'-hydroxybenzimidamide[40] (0.073 g, 0.43 mmol) was dissolved in DMSO (0.5 mL). Powdered NaOH (0.026 g, 0.63 mmol) was added at once and the reaction mixture was stirred at room temperature for 7 hours monitored by TLC. Water (8 mL) was added and the reaction mixture was stirred for 15 minutes after which the precipitate was collected by filtration and washed with water (15 mL). The solid was dried *in vacuo* and purified by recrystallization from EtOAc (7 mL) and dried *in vacuo* and freeze dried. The product was isolated as a white solid (0.103 g, 64%

yield): mp 242 °C. R_f = 0.8 (DCM : MeOH) (10 : 1). R_t = 14.55 min (>98% pure by HPLC 2). This sample was dissolved in 1.0 mL of DMSO. ^{1}H NMR (400 MHz, Chloroform-*d*) δ 9.70 (d, *J* = 6.9 Hz, 1H), 8.13 (d, *J* = 8.4 Hz, 2H), 7.93 – 7.89 (m, 2H), 7.86 (d, *J* = 9.0 Hz, 1H), 7.59 – 7.44 (m, 6H), 7.20 (t, *J* = 6.9 Hz, 1H). ^{13}C NMR (151 MHz, Chloroform-*d*) δ 168.53, 167.21, 152.70, 147.60, 137.69, 132.80, 129.93, 129.78, 129.41, 129.01, 128.76, 128.49, 128.31, 125.32, 117.85, 114.91, 107.54. ESI-MS (m/z) calculated $[M + H]$ for $C_{21}H_{14}ClN_4O$ =373.09, found 373.1 and $[M + 2 + H]^+$ = 375.1.

Computational chemistry

Homology model

The model was built using the Maestro Schrödinger, package version 10.7.015, release 2016-3, using *Prime, Structure Prediction Wizard*. The 3.86Å cryoEM structure of the human $GABA_AR$ $\alpha_1\beta_2\gamma_2$ heteropentamer in complex with GABA and flumazenil (PDB-code: 6D6T) was used as a template for this ECD homology model. The human sequences of the ECDs of the α_4- and δ-subunits (Entries and P48169 and O14764) were extracted from the UniProt database[57] and aligned with the template (Chain D α_1-subunit and Chain E γ_2-subunit, respectively), using *ClustalW* within Maestro.

The Residues 36-43 of the α_4-subunit and the residues 17-39 of the δ-subunit were deleted as they were poorly modeled due to lack of a template and expected to be far from the C-loop binding pocket, based on the built monomers. The sequence identities of the ECD of the α_4- and δ-subunits to the templates were found to be 69% and 36%, respectively.

The model was initially built as monomers using the energy-based method. The monomers were then combined into a heterodimer, using the *Prime Multimer function*. The heterodimer were then prepared using the *Protein Preparation Wizard*, to fix problems such as steric clashes.

The expected protonation state of the amino acid residues at pH = 7.4 was then calculated using *PropKa*. Afterwards, the model was energy-minimized using *OPLS3* force fields.

The model was assessed by *ProCheck*[58] in which it was found that 88.9%, 10.6% and 0.5% of the modeled amino acid residues were in most favored regions, additional allowed regions and generously allowed regions, respectively (Supporting information). The outliers in the Ramachandran plot, the residues GLU72(A) and GLN162(B) were visually inspected and found to be nowhere near the binding site of investigation.

Docking

The ligands were manually drawn within Maestro (Release 2016-3: Maestro, Schrödinger, LLC, New York, NY, 2016) and preprocessed using *LigPrep* (Release 2016-3: LigPrep, Schrödinger, LLC, New York, NY, 2016), the structures were energy minimized using *OPLS3* forced fields. Protonation state of the ligands was determined by *Epik* at pH =7.4±2.

To ensure a binding model that can encompasse analogues of different sizes from the previous publication[17] the relatively large 4-butoxy-*N*-(6-chloro-2-(thiophen-2-yl)imidazo[1,2-*a*]pyridin-3-yl)benzamide were initially docked using induced fit docking (Release 2016-3: Induced Fit Docking protocol; Glide & Prime, Schrödinger, LLC, New York, NY, 2016). The calculations were performed with the *OPLS3* force fields, Xtra Precision (XP) Glide for redocking and the centroid of the box was specified from the residues, α_4R135 and δF90; otherwise, default settings were applied. Among the very similar three top-ranked poses according to the IFD score we selected the pose with the best Emodel score. The ligand was deleted and the resulting protein was used as a docking template for XP docking (Release 2016-3: Glide, Schrödinger, LLC, New York, NY, 2016) of a selection of analogoues, i.e. (*N*-(6-bromo-2-(thiophen-2-yl)imidazo[1,2-*a*]pyridin-3-yl)-4-methoxybenzamide, *N*-(6,8-dibromo-2-(thiophen-2-yl)imidazo[1,2-*a*]pyridin-3-yl)-4-methoxybenzamide, 4-butoxy-*N*-(6-chloro-2-(thiophen-2-yl)imidazo[1,2-*a*]pyridin-3-yl)benzamide and DS2. The DS2 pose with the

best Emodel displayed a binding mode consistent with high scoring poses of the other compounds and were selected for design of new compounds.

Pharmacology

Compounds

GABA and DS2 (4-chloro-N-[2-(2-thienyl)imidazo[1,2-a]pyridin-3-yl]benzamide) were obtained from Tocris Bioscience (Bristol, UK).

Cell culturing and transient transfection

All used HEK293 cell lines were maintained in DMEM containing Gluta-MAX-I supplemented with 10% Fetal bovine serum (FBS) and 1% penicillin-streptomycin (all from Life Technologies, Paisley, UK) in an incubator at 37°C with a humidity of 5% CO_2. The HEK293 Flp-In cell line stably expressing the human δ-subunit (δ-HEK) and the background HEK cell line stably expressing the G-protein coupled receptor NPBWR2 were positively selected using 200 μg/mL hygromycin B as reported previously[59].

Recombinant human $\alpha_4\beta_1\delta$ and $\alpha_4\beta_1\gamma_2$ $GABA_A$-receptors were expressed by transfection of δ-HEK cells and HEK background cells, respectively. δ-HEK cells were transfected in a 1:1 ratio of human α_4- and β_1-subunits (pUNIV) to express $\alpha_4\beta_1\delta$. HEK background cells were transfected in a 1:1:2 ratio of human α_4-, β_1- and γ_2-subunit (pcDNA3.1/Zeo) to express $\alpha_4\beta_1\gamma_2$ using Polyfect transfection reagent (Qiagen, West Sussex, UK) as described by the manufacturer, except for using half volumes. A cell line stably expressing $\alpha_1\beta_2\gamma_2$ receptors in HEK293 cells as previously used[59] was a gift from Marianne L. Jensen, Neurosearch.

FLIPR membrane potential (FMP) assay

Testing of compounds in the fluorescence-based FMP assay was performed exactly as described previously.[59] Data was obtained as relative changes in fluorescence units (ΔRFU) given as the difference between the baseline fluorescence signal before compound addition and the peak/top plateau in the fluorescence signal obtained after buffer/compound addition. All raw data traces were inspected manually and signals resulting from buffer/compound addtions and signal artefacts were omitted from the analysis.

For agonist testing, the obtained ΔRFU responses were normalized to the ΔRFU response induced by 100 μM GABA (maximum reponse) after subtraction of the buffer response and given as %Response of $GABA_{max}$. When testing for PAM effect, the analogs were co-applied with a concentration of GABA corresponding to approximately GABA EC_{20} valuesdetermined from full GABA concentration-response curves at the respective receptor subtypes (see Table 2). The obtained ΔRFU responses were normalized to the ΔRFU response induced by 100 μM GABA (maximum reponse) after subtraction of the buffer response and given as %Response of $GABA_{max}$.

Concentration-response curves used to determine the PAM potencies (EC_{50}-values) of the analogs and the agonist potencies of GABA used to determined GABA EC_{20} values were fitted to the four-parameter concentration-response model:

$$\text{Response} = \text{bottom} + \frac{\text{top-bottom}}{1+10^{[(\log EC_{50}\text{-}A)\cdot n_H]}}$$

where EC_{50} is the concentration of the compound A resulting in the half-maximum response (reponse halfway between top and bottom) and n_H is the Hill coefficent of the curve. The data analysis was performed using GraphPad Prism v. 8.4.3 (GraphPad software Inc., San Diego, CA, USA).

ASSOCIATED CONTENT

Supporting information. The following files are available free of charge.

Supplementary docking information

Molecular formula string (CSV)

AUTHOR INFORMATION

Corresponding Author

*Bente Frølund. Department of Drug Design and Pharmacology, University of Copenhagen, Jagtvej 162, 2100 København Ø, Denmark. ORCID**:** 0000-0001-5476-6288; +45 35336495; bfr@sund.ku.dk

Author Contributions

The manuscript was written through contributions of all authors. F.R. and K.H. performed the modeling studies. F.R., I.C. and S.J. synthesized the compounds. C.F.P., S.B. and P.W. performed FMP assays. B.N. performed radioligand binding assay. B.F. devised the study and supervised the work. All authors have given approval to the final version of the manuscript.

ACKNOWLEDGMENT

This work was supported by a Lundbeck Foundation (grant R230-2016-2562 to C.B.F.-P.) and the Drug Research Academy.

ABBREVIATIONS

GABA, γ-aminobutyric acid; $GABA_ARs$, γ-aminobutyric acid type A receptors; PAM, positive allosteric modulator; [^{3}H]-EBOB, [^{3}H]-ethynylbicyclooethobenzoate; SAR, structure-activity relationship; ECD, extracellular domain, CryoEM, Cryogenic Electron Microscopy; FMP, FLIPR Membrane Potential; XP, Xtra precision; SEM, Standard Error of the Mean;

REFERENCES

1. David, F. O.; Arnold, R. K. Is there more to gaba than synaptic inhibition? *Nature Rev. Neurosci.* **2002,** *3*, 715–727.

2. Tija C, J.; Guido, M. GABAA receptor trafficking and its role in the dynamic modulation of neuronal inhibition. *Nature Rev. Neurosci.* **2008**, *9*, 331–343.

3. Chiara, D. C.; Jounaidi, Y.; Zhou, X.; Savechenkov, P. Y.; Bruzik, K. S.; Miller, K. W.; Cohen, J. B. General Anesthetic Binding Sites in Human α4β3δ γ-Aminobutyric Acid Type A Receptors (GABAARs). *J. Biol. Chem.* **2016,** *291*, 26529–26539.

4. Hanson, S. M.; Czajkowski, C. Structural mechanisms underlying benzodiazepine modulation of the GABA(A) receptor. *J. Neurosci.* **2008,** *28*, 3490–3499.

5. Möhler, H.; Fritschy, J. M.; Rudolph, U. A New Benzodiazepine Pharmacology. *J. Pharmacol. Exp. Ther.* **2002,** *300*, 2–8.

6. Gravielle, M. C. Regulation of GABAA receptors by prolonged exposure to endogenous and exogenous ligands. *Neurochem. Intern.* **2018,** *118*, 96-104.

7. Farrant, M.; Nusser, Z. Variations on an inhibitory theme: phasic and tonic activation of GABAA receptors. *Nature Rev. Neurosci.* **2005,** *6*, 215–229.

8. Chuang, S.-H.; Reddy, D. S. Genetic and Molecular Regulation of Extrasynaptic GABA-A Receptors in the Brain: Therapeutic Insights for Epilepsy. *J. Pharmacol. Exp. Ther.* **2018,** *364*, 180–197.

9. Roberto, M.; Varodayan, F. P. Synaptic targets: Chronic alcohol actions. *Neuropharmacol.* **2017,** *122*, 85-99.

10. Holm, M. M.; Nieto-Gonzalez, J. L.; Vardya, I.; Henningsen, K.; Jayatissa, M. N.; Wiborg, O.; Jensen, K. Hippocampal GABAergic dysfunction in a rat chronic mild stress model of depression. *Hippocampus* **2011,** *21*, 422–433.

11. Brickley, S. G.; Mody, I. Extrasynaptic GABA(A) receptors: their function in the CNS and implications for disease. *Neuron* **2012,** *73*, 23–34.

12. Lee, V.; Maguire, J. The impact of tonic GABAA receptor-mediated inhibition on neuronal excitability varies across brain region and cell type. *Front Neural Circuits* **2014,** *8*, 1–27.

13. Solomon, V. R.; Tallapragada, V. J.; Chebib, M.; Johnston, G. A. R.; Hanrahan, J. R. GABA allosteric modulators: An overview of recent developments in non-benzodiazepine modulators. *Eur. J. Med. Chem.* **2019,** *171*, 434–461.

14. Lee, H. J.; Absalom, N. L.; Hanrahan, J. R.; van Nieuwenhuijzen, P.; Ahring, P. K.; Chebib, M. A pharmacological characterization of GABA, THIP and DS2 at binary alpha4beta3 and beta3delta receptors: GABA activates beta3delta receptors via the beta3(+)delta(-) interface. *Brain Res.* **2016,** *1644*, 222–230.

15. Jensen, M. L.; Wafford, K. A.; Brown, A. R.; Belelli, D.; Lambert, J. J.; Mirza, N. R. A study of subunit selectivity, mechanism and site of action of the delta selective compound 2 (DS2) at human recombinant and rodent native GABAA receptors. *Br. J. Pharmacol.* **2013,** *168*, 1118–1132.

16. L'Estrade, E. T.; Hansen, H. D.; Falk-Petersen, C.; Haugaard, A.; Griem-Krey, N.; Jung, S.; Lüddens, H.; Schirmeister, T.; Erlandsson, M.; Ohlsson, T.; Knudsen, G. M.; Herth, M. M.; Wellendorph, P.; Frølund, B. Synthesis and Pharmacological Evaluation of [11C]4-Methoxy-N-[2-(thiophen-2-yl)imidazo[1,2-a]pyridin-3-yl]benzamide as a Brain Penetrant PET Ligand Selective for the δ-Subunit-Containing γ-Aminobutyric Acid Type A Receptors. *ACS Omega* **2019,** *4*, 8846–8851.

17. Yakoub, K.; Jung, S.; Sattler, C.; Damerow, H.; Weber, J.; Kretzschmann, A.; Cankaya, A. S.; Piel, M.; Rösch, F.; Haugaard, A. S.; Frølund, B.; Schirmeister, T.; Lüddens, H. Structure–Function Evaluation of Imidazopyridine Derivatives Selective for δ-Subunit-Containing γ-Aminobutyric Acid Type A (GABAA) Receptors. *J. Med. Chem.* **2018,** *61*, 1951–1968.

18. Cole, L. M.; Casida, J. E. GABA-gated chloride channel: binding-site for 4'-ethynyl-4-n-[2,3-3H2]propylbicycloorthobenzoate. *Pestic. Biochem. Physiol.* **1992,** *44*, 1–8.

19. Uusi-Oukari, M.; Maksay, G. Allosteric modulation of [3H]EBOB binding to GABAA receptors by diflunisal analogues. *Neurochem. Int.* **2006,** *49*, 676–682.

20. Yagle, M. A.; Martin, M. W.; de Fiebre, C. M.; de Fiebre, N. C.; Drewe, J. A.; Dillon, G. H. [3H]Ethynylbicycloorthobenzoate ([3H]EBOB) binding in recombinant GABAA receptors. *Neurotoxicol.* **2003,** *24*, 817–824.

21. Maksay, G.; Biro, T. High affinity, heterogeneous displacement of [3H]EBOB binding to cerebellar GABA A receptors by neurosteroids and GABA agonists. *Neuropharmacol.* **2005,** *49*, 431–438.

22. Stephen, G. B.; Zhiwen, E.; Thomas, P. M.; Catriona, M. H. The contribution of delta subunit-containing GABAA receptors to phasic and tonic conductance changes in cerebellum, thalamus and neocortex. *Frontiers in Neural Circuits* **2013**, *7*, 1–8.

23. Hartiadi, L. Y.; Ahring, P. K.; Chebib, M.; Absalom, N. L. High and low GABA sensitivity α4β2δ GABAA receptors are expressed in Xenopus laevis oocytes with divergent stoichiometries. *Biochem. Pharmacol.* **2016**, *103*, 98–108.

24. Masiulis, S.; Desai, R.; Uchański, T.; Serna Martin, I.; Laverty, D.; Karia, D.; Malinauskas, T.; Zivanov, J.; Pardon, E.; Kotecha, A.; Steyaert, J.; Miller, K. W.; Aricescu, A. R. GABAA receptor signalling mechanisms revealed by structural pharmacology. *Nature* **2019,** *565*, 454–459.

25. Ahring, P. K.; Bang, L. H.; Jensen, M. L.; Strøbæk, D.; Hartiadi, L. Y.; Chebib, M.; Absalom, N. A pharmacological assessment of agonists and modulators at α4β2γ2 and α4β2δ GABAA receptors: The challenge in comparing apples with oranges. *Pharmacol. Res.* **2016,** *111*, 563–576.

26. Kaur, K. H.; Baur, R.; Sigel, E. Unanticipated structural and functional properties of delta-subunit-containing GABAA receptors. *J. Biol.Chem.* **2009,** *284*, 7889–7896.

27. Baur, R.; Kaur, K.; Sigel, E. Structure of alpha6 beta3 delta GABAA receptors and their lack of ethanol sensitivity. *J. Neurochem.* **2009,** *111*, 1172–1181.

28. Barrera, N. P.; Betts, J.; You, H.; Henderson, R. M.; Martin, I. L.; Dunn, S. M. J.; Edwardson, J. M. Atomic force microscopy reveals the stoichiometry and subunit arrangement of the alpha4beta3delta GABA(A) receptor. *Mol.Pharmacol.* **2008,** *73*, 960–967.

29. Patel, B.; Mortensen, M.; Smart, T. G. Stoichiometry of δ subunit containing GABAA receptors. *Br. J. Pharmacol.* **2014,** *171*, 985–994.

30. Zhu, S.; Noviello, C. M.; Teng, J.; Walsh, R. M.; Kim, J. J.; Hibbs, R. E. Structure of a human synaptic GABAA receptor. *Nature* **2018,** *559*, 67–72.

31. Bienaymé, H.; Bouzid, K. A New Heterocyclic Multicomponent Reaction For the Combinatorial Synthesis of Fused 3-Aminoimidazoles. *Ang. Chem. Int. Ed.* **1998,** *37*, 2234–2237.

32. Groebke, K.; Weber, L.; Mehlin, F. Synthesis of Imidazo[1,2-a] annulated Pyridines, Pyrazines and Pyrimidines by a Novel Three-Component Condensation. *Synlett* **1998,** *6*, 661-663.

33. Blackburn, C.; Guan, B.; Fleming, P.; Shiosaki, K.; Tsai, S. Parallel synthesis of 3-aminoimidazo[1,2-a]pyridines and pyrazines by a new three-component condensation. *Tetrahedron Lett.* **1998,** *39*, 3635–3638.

34. Guchhait, S. K.; Chaudhary, V.; Madaan, C. A chemoselective Ugi-type reaction in water using TMSCN as a functional isonitrile equivalent: generation of heteroaromatic molecular diversity. *Org. Biomol. Chem.* **2012,** *10*, 9271–9277.

35. Bazin, M.-A.; Marhadour, S.; Tonnerre, A.; Marchand, P. Exploration of versatile reactions on 2-chloro-3-nitroimidazo[1,2-a]pyridine: expanding structural diversity of C2- and C3-functionalized imidazo[1,2-a]pyridines. *Tetrahedron Lett.* **2013,** *54*, 5378–5382.

36. Misra, A. P.; Raj, K.; Bhaduri, A. P. In Search of Imidazo [1,2-a] Pyridine Derivatives Exhibiting Resistance for Catalytic Hydrogenation. *Synth. Comm.* **1999,** *29*, 3227–3236.

37. Tokuhara, H.; Imaeda, Y.; Fukase, Y.; Iwanaga, K.; Taya, N.; Watanabe, K.; Kanagawa, R.; Matsuda, K.; Kajimoto, Y.; Kusumoto, K.; Kondo, M.; Snell, G.; Behnke, C. A.; Kuroita, T. Discovery of benzimidazole derivatives as orally active renin inhibitors: Optimization of 3,5-disubstituted piperidine to improve pharmacokinetic profile. *Bioorg. Med. Chem.* **2018,** *26*, 3261–3286.

38. El Akkaoui, A.; Bassoude, I.; Koubachi, J.; Berteina-Raboin, S.; Mouaddib, A.; Guillaumet, G. Pd-catalyzed regiocontrolled Sonogashira and Suzuki cross-coupling reaction of 3,6-dihalogenoimidazo[1,2-a]pyridines: one-pot double-coupling approach. *Tetrahedron* **2011,** *67*, 7128-7138.

39. Huo, C.; Tang, J.; Xie, H.; Wang, Y.; Dong, J. CBr4 Mediated Oxidative C–N Bond Formation: Applied in the Synthesis of Imidazo[1,2-α]pyridines and Imidazo[1,2-α]pyrimidines. *Org. Lett.* **2016,** *18*, 1016–1019.

40. Mayer, J.; Sauer, A.; Iglesias, B. A.; Acunha, T. V.; Back, D.; Rodrigues, O.; Dornelles, L. Ferrocenylethenyl-substituted 1,3,4-oxadiazolyl-1,2,4-oxadiazoles: Synthesis, characterization and DNA-binding assays. *J. Organometal. Chem.* **2017,** *841*, 1–11.

41. Schwartz, T. W.; Holst, B. Allosteric enhancers, allosteric agonists and ago-allosteric modulators: where do they bind and how do they act? *Trends Pharmacol. Sci.* **2007,** *28*, 366–373.

42. Madjroh, N.; Olander, E. R.; Bundgaard, C.; Soderhielm, P. C.; Jensen, A. A. Functional properties and mechanism of action of PPTQ, an allosteric agonist and low nanomolar positive allosteric modulator at GABAA receptors. *Biochem. Pharmacol.* **2018,** *147*, 153–169.

43. Gill, J. K.; Dhankher, P.; Sheppard, T. D.; Sher, E.; Millar, N. S. A series of alpha7 nicotinic acetylcholine receptor allosteric modulators with close chemical similarity but diverse pharmacological properties. *Mol. Pharmacol.* **2012,** *81*, 710–718.

44. Dalby, N. O.; Falk-Petersen, C. B.; Leurs, U.; Scholze, P.; Krall, J.; Frolund, B.; Wellendorph, P. Silencing of spontaneous activity at alpha4beta1/3delta GABAA receptors in hippocampal granule cells reveals different ligand pharmacology. *Br. J. Pharmacol.* **2020**, *177*, 3975–3990.

45. Martínez-Urbina, M. A.; Zentella, A.; Vilchis-Reyes, M. A.; Guzmán, Á.; Vargas, O.; Ramírez Apan, M. T.; Ventura Gallegos, J. L.; Díaz, E. 6-Substituted 2-(N-trifluoroacetylamino)imidazopyridines induce cell cycle arrest and apoptosis in SK-LU-1 human cancer cell line. *Eur. J. Med. Chem.* **2010,** *45*, 1211–1219.

46. Schwerkoske, J.; Masquelin, T.; Perun, T.; Hulme, C. New multi-component reaction accessing 3-aminoimidazo[1,2-a]pyridines. *Tetrahedron Lett.* **2005,** *46*, 8355–8357.

47. Yan, R.-L.; Yan, H.; Ma, C.; Ren, Z.-Y.; Gao, X.-A.; Huang, G.-S.; Liang, Y.-M. Cu(I)-Catalyzed Synthesis of Imidazo[1,2-a]pyridines from Aminopyridines and Nitroolefins Using Air as the Oxidant. *J. Org. Chem.* **2012,** *77*, 2024–2028.

48. Reynoso Lara, J. E.; Salgado-Zamora, H.; Bazin, M.-A.; Campos-Aldrete, M. E.; Marchand, P. Design and Synthesis of Imidazo[1,2-a]pyridines with Carboxamide Group Substitution and In

silico Evaluation of their Interaction with a LuxR-type Quorum Sensing Receptor. *J. Heterocycl. Chem.* **2018,** *55*, 1101–1111.

49. Kour, D.; Khajuria, R.; Kapoor, K. Iodine-ammonium acetate promoted reaction between 2-aminopyridine and aryl methyl ketones: a novel approach towards the synthesis of 2-arylimidazo[1,2-a]pyridines. *Tetrahedron Lett.* **2016,** *57*, 4464–4467.

50. Sayeed, I. B.; Lakshma Nayak, V.; Shareef, M. A.; Chouhan, N. K.; Kamal, A. Design, synthesis and biological evaluation of imidazopyridine–propenone conjugates as potent tubulin inhibitors. *Med. Chem. Comm.* **2017,** *8*, 1000–1006.

51. Salgado-Zamora, H.; Velazquez, M.; Mejía, D.; Campos-Aldrete, M. E.; Jimenez, R.; Cervantes, H. Influence of the 2-aryl group on the ipso electrophilic substitution process of 2-arylimidazo[1,2-a]pyridines. *Heterocycl. Comm.* **2008,** *14*, 27–32.

52. Zhou, X.; Yan, H.; Ma, C.; He, Y.; Li, Y.; Cao, J.; Yan, R.; Huang, G. Copper-Mediated Aerobic Oxidative Synthesis of 3-Bromo-imidazo[1,2-a]pyridines with Pyridines and Enamides. *J. Org. Chem.* **2016,** *81*, 25–31.

53. Delaye, P. O.; Pnichon, M.; Allouchi, H.; Enguehard-Gueiffier, C.; Gueiffier, A. Regiocontrolled functionalization of 2,3-dihalogenoimidazo[1,2- a]pyridines by SuzukiMiyaura and Sonogashira cross-coupling reactions. *Org. Biomol. Chem.* **2017,** *15*, 4199–4204.

54. Ganguly, B.; Kar, B.; Dwivedi, S.; Das, S. Green procedure for highly efficient, rapid synthesis of imidazo[1,2-a]pyridine and its late stage functionalization AU - Ghosh, Prasanjit. *Synth. Comm.* **2018,** *48*, 1076–1084.

55. Zhang, Y.; Chen, Z.; Wu, W.; Zhang, Y.; Su, W. CuI-Catalyzed Aerobic Oxidative α-Aminaton Cyclization of Ketones to Access Aryl or Alkenyl-Substituted Imidazoheterocycles. *J. Org. Chem.* **2013,** *78*, 12494–12504.

56. Chen, Z.; Cao, G.; Zhang, F.; Li, H.; Xu, J.; Miao, M.; Ren, H. Metal-Free Mediated C-3 Methylsulfanylation of Imidazo[1,2-a]-pyridines with Dimethyl Sulfoxide as a Methylsulfanylating Agent. *Synlett* **2017,** *28*, 1795–1800.

57. The UniProt, C. UniProt: a worldwide hub of protein knowledge. *Nucl. Acids Res.* **2018,** *47*, D506–D515.

58. R. A. Laskowski, M. W. M., D. S. Moss and J. M. Thornton. PROCHECK: a program to check the stereochemical quality of protein structures. *J. Appl. Crystallography* **1993,** *26*, 283–291.

59. Falk-Petersen, C. B.; Søgaard, R.; Madsen, K. L.; Klein, A. B.; Frølund, B.; Wellendorph, P. Development of a Robust Mammalian Cell-based Assay for Studying Recombinant α β δ GABA Receptor Subtypes. *Basic Clinical Pharmacol. Tox.* **2017,** *121*, 119–129.

Table of Contents graphics